

1 This is the peer-reviewed version of the following article:
2

3 *The Journal of Physical Chemistry B* **2015**, *119*, 2475–2489, DOI: 10.1021/jp507917u, which has been
4 published in final form at <https://pubs.acs.org/doi/abs/10.1021/jp507917u>.
5
6

7 This article may be used for non-commercial purposes only.
8
9
10
11
12
13
14
15
16
17
18
19
20

21
22 **Excited-State Proton and Charge Transfer in**
23
24
25
26 **Protonated Amino and Methylated Derivatives of**
27
28
29
30 **2-(2'-Hydroxyphenyl)benzimidazole**
31
32
33

34 *Sonia Ríos Vázquez, J. Luis Pérez Lustres, Flor Rodríguez-Prieto,* Manuel Mosquera,* and M.*

35
36 *Carmen Ríos Rodríguez**
37
38

39
40 Departamento de Química Física and Centro Singular de Investigación en Química Biolóxica e
41
42 Materiais Moleculares (CIQUS), Universidade de Santiago de Compostela, E-15782 Santiago de
43
44 Compostela, Spain.
45
46
47
48
49
50
51
52
53
54
55
56
57
58
59
60

ABSTRACT: We studied the excited-state behavior of a family of mono- and diprotonated derivatives of 2-phenylbenzimidazole in different solvents, using steady-state and time-resolved fluorescence spectroscopy. The species investigated were 2-(4'-amino-2'-hydroxyphenyl)benzimidazole (**1**), the diethylamino analogue 2-(4'-*N,N*-diethylamino-2'-hydroxyphenyl)benzimidazole (**2**) and its *N*-methylated derivative 1-methyl-2-(4'-*N,N*-diethylamino-2'-hydroxyphenyl)benzimidazole (**3**). The *O*-methoxy derivatives of **2** and **3** (**2-OMe** and **3-OMe**), and the simpler models 2-phenylbenzimidazole (**4**) and its 4'-amino (**5**) and 4'-dimethylamino (**6**) derivatives were also studied. We found that the dications of **1**, **2**, and **3** (protonated at the benzimidazole N3 and at the amino group) were strong photoacids, which were deprotonated at the hydroxyl group upon excitation in aqueous solution (totally for **2** and **3**) to give a tautomer of the ground-state monocation. In contrast, no photodissociation was observed for the monocations of these species. Instead, some of the monocations studied behaved as molecular rotors, for which electronic excitation led to a twisted intramolecular charge transfer (TICT) state. The monocations of **2**, **3**, **2-OMe**, **3-OMe**, and **6**, protonated at the benzimidazole N3, experienced a polarity- and viscosity-dependent radiationless deactivation associated to a large-amplitude rotational motion. We propose that this process is connected to an intramolecular charge transfer from the dimethylaminophenyl or diethylaminophenyl moiety (donor) to the protonated benzimidazole group (acceptor) of the excited monocation, which yields a twisted charge-transfer species. No fluorescence from this species was detected except for **3** and **3-OMe** in low-viscosity solvents.

Keywords: Photoacidity. Photodissociation. Molecular rotor. TICT state.

1. INTRODUCTION

Proton- and electron-transfer reactions, frequently coupled, play a crucial role in many essential processes taking place in living organisms, like DNA chemical damage and repair,^{1,2} photostability of DNA base pairs and proteins,³ photosynthesis,⁴ and respiration.⁵ Although these reactions have been extensively investigated, the detailed mechanisms of charge transfer and proton motion, and in particular the coupling between them, are not completely understood.⁶⁻¹¹

Photoinduced proton- and electron-transfer processes are triggered by the change of acid–base and redox properties of molecules upon electronic excitation. Molecules with both electron donor and acceptor moieties often undergo in the excited state a photoinduced intramolecular electron transfer. These systems have applications as luminescence sensors,¹² in organic solar cells^{13,14} or in light-driven molecular machines.¹⁵

Molecules with increased acidity in the excited state are called photoacids, as they have the tendency to be deprotonated upon excitation in solvents capable of accepting the proton or in the presence of basic species. Recent research on photoacids has greatly contributed to our understanding of the elementary steps in proton-transfer processes.¹⁶⁻¹⁹ Photoacids have also found applications as polymerization initiators,²⁰ in molecular machines²¹ and in pH-jump experiments.²² If a molecule has an acid group and a basic site linked by a hydrogen bond in the ground state, an ultrafast excited-state intramolecular proton transfer, ESIPT, from the acid to the basic site may occur. ESIPT molecules have technological applications as UV photostabilizers,²³ and are potential components for photoswitches²⁴ and organic LEDs.²⁵

2-(2'-hydroxyphenyl)benzimidazole (HBI),²⁶⁻⁴⁰ 2-(4'-amino-2'-hydroxyphenyl)benzimidazole (**1**),^{36,41,42} 2-(4'-*N,N*-diethylamino-2'-hydroxyphenyl)benzimidazole (**2**),^{36,41} 1-methyl-2-(4'-*N,N*-diethylamino-2'-hydroxyphenyl)benzimidazole (**3**),⁴¹ and 2-(3'-hydroxy-2'-

1
2
3 pyridyl)benzimidazole^{43,44} are examples of ESIPT molecules studied in our group (see Chart 1).
4
5 A solvent-modulated ground-state rotameric and tautomeric equilibrium was observed for these
6
7 benzimidazole derivatives. In apolar aprotic solvents, these compounds exist in the ground state
8
9 as the planar *syn* normal form N_{syn} (Chart 1), with an intramolecular hydrogen bond $N\cdots H-O$.
10
11 This species undergoes in the first-excited singlet state an intramolecular proton transfer from the
12
13 hydroxyl group to the benzimidazole N3 to yield the excited **T** tautomer (see in Chart 1 the
14
15 limiting resonance structures of this species). In protic solvents, a ground-state rotameric
16
17 equilibrium between N_{syn} and its planar *anti* rotamer N_{anti} was detected for HBI,^{31,32,34} **1**, and **2**,
18
19 and between N_{syn} and a non-planar N_{np} rotamer for the sterically hindered compound **3** (Chart
20
21 **1**).⁴¹ N_{anti} and N_{np} , unable to undergo ESIPT, yield normal N^* emission upon excitation. Water
22
23 stabilizes the ground-state **T** tautomer, which was detected by its red-shifted absorption in
24
25 aqueous solutions of HBI, **1**, **2** and **3**.^{34,41}
26
27
28
29
30
31

32 Whereas the fluorescence quantum yield and lifetime of T^* showed for HBI no dependence
33
34 on solvent or temperature,⁴⁵ those of the tautomers of **2** and **3** revealed a temperature-, polarity-
35
36 and viscosity-dependent radiationless deactivation connected with a large-amplitude
37
38 conformational motion occurring for these HBI derivatives.⁴¹ We have shown that this
39
40 conformational change is associated with a charge transfer experienced by T^* from the
41
42 deprotonated dialkylaminophenol group (donor) to the protonated benzimidazole group
43
44 (acceptor), affording a non-fluorescent charge-transfer structure T_{ct}^* .⁴¹ This excited-state
45
46 intramolecular proton-coupled charge-transfer process was reported by us for 2-(2'-
47
48 hydroxyphenyl)benzoxazole, 2-(2'-hydroxyphenyl)benzothiazole, and other
49
50 hydroxyarylbenzazoles in solution, but we did not observe it for HBI.⁴⁵ We demonstrated that the
51
52 efficiency of this process increased with the electron-donor strength and with the steric hindrance
53
54
55
56
57
58
59
60

1
2
3 caused by N1-methylation, and decreased as the solvent viscosity was increased. Theoretical
4
5 calculations performed later by Tsai et al.³⁶ on HBI, **1** and **2** predict that two different charge-
6
7 transfer states are stable in ethanol and cyclohexane for these compounds. Recently reported
8
9 investigations³⁷ on ESIPT in crystal structures of HBI polymorphs (α and β) showed that the
10
11 tautomer form of polymorph β undergoes in the excited state an intramolecular charge transfer
12
13 process which does not occur for polymorph α , this revealing the importance of intermolecular
14
15 interactions for the relative stability of **T*** and its charge-transfer form. In a poly(methyl
16
17 methacrylate) film, the polarizability of HBI tautomer was found to be smaller in S_1 than in S_0 ,
18
19 suggesting a twisted geometry for **T** in S_1 .³⁸ Molecules showing a viscosity-dependent
20
21 fluorescence lifetime due to an intramolecular twisting occurring in the excited state are
22
23 molecular rotors. These fluorescent molecular rotors can be employed as reporters of the local
24
25 microviscosity, in particular in live cells, by fluorescence lifetime imaging.^{46,47}

26
27
28
29
30
31
32 We found that the monocations of HBI,³⁴ 2-(3'-hydroxy-2'-pyridyl)benzimidazole,⁴⁸ and 2-
33
34 (1'-hydroxy-2'-naphthyl)benzimidazole,^{19,49} protonated at the benzimidazole N3, are strong
35
36 photoacids, which become completely deprotonated at the OH group in aqueous solution and to a
37
38 great extent in short-chain alcohols. It is interesting to investigate the effect of the electron-
39
40 donating substituents at the phenol group on the photoacid properties of this class of compounds.
41
42 The amino groups of **1**, **2**, and **3** act as electron donors, but this effect disappears when they are
43
44 protonated. We will study the influence of a protonated or non-protonated amino group on the
45
46 photoacid behavior for the monocations (**MC**, see Chart 2) and dications (**DC**) of **1**, **2**, and **3**.

47
48
49
50
51 If we compare the monocations of **1**, **2**, and **3** (Chart 2) with the structure of the neutral
52
53 tautomer **T** (Chart 1), we observe that they have the same electron acceptor (protonated
54
55 benzimidazole), but the monocations have a weaker electron donor (aminophenol instead of
56
57
58
59
60

1
2
3 aminophenoxy group). Therefore, it is also possible that the excited monocations undergo a
4 charge-transfer process from the aminophenol group to the protonated benzimidazole moiety.
5
6 This process is also possible for the monocations of **2-OMe** and **3-OMe** (Chart 2). In contrast,
7
8 the dications of **1**, **2**, **3**, **2-OMe**, and **3-OMe**, protonated both at the benzimidazole N3 and at the
9
10 amino group, are not expected to undergo the photoinduced charge transfer process, as the
11
12 protonated aminophenol moiety is not a good electron donor. Therefore, it is interesting to
13
14 compare the behavior of monocations and dications of the mentioned species, to investigate the
15
16 existence of the intramolecular charge-transfer process.
17
18
19
20
21

22 In this paper, we present a study of the ground- and excited-state behavior of the monocations
23 and dications of **1**, **2**, and **3**, in different acidified protic and aprotic solvents. We report the
24 room-temperature fluorescence of **1**, **2**, and **3** in acidified solvents of various viscosities and
25 polarities and compare it with the fluorescence of the methoxy derivatives **2-OMe** and **3-OMe**
26 (Chart 2), unable to deprotonate under excitation, but prone to undergo a charge-transfer process
27 in the excited state. Moreover, we investigated the fluorescence of the monocations of simple
28 models phenylbenzimidazole (**4**, Chart 2), p-aminophenylbenzimidazole (**5**), and
29 p-dimethylaminophenylbenzimidazole (**6**), sharing the same electron acceptor, but with different
30 electron donors.
31
32
33
34
35
36
37
38
39
40
41
42

43 The aims of the present study were (1) to find out if the monocations and dications of **1**, **2**,
44 and **3** deprotonate in the excited state in protic solvents, and (2) to examine if these compounds
45 and the related species shown in Chart 2 undergo in the excited state a large-amplitude
46 conformational motion connected to an intramolecular charge migration analogous to that
47 observed for the neutral tautomer **T***.
48
49
50
51
52
53
54
55
56
57
58
59
60

2. EXPERIMENTAL SECTION

2.1. Materials. HBI³⁴ and **1**, **2**, **3**, **2-OMe**, and **3-OMe**⁴¹ were synthesized as described elsewhere. **4** was provided by Aldrich.

Compound **5** was prepared by condensation of 20 mmol of 1,2-benzenediamine (Aldrich) with 20 mmol of 4-aminobenzoic acid (Aldrich) at ~ 100 °C for 24 h. The solid obtained was dissolved in acetone and the product precipitated by adding water. ¹H NMR (300 MHz, DMSO), δ (ppm): 5.58 (s, 2H), 6.65 (d, 2H, $J = 8.8$ Hz), 7.10 (dd, 2H, $J = 6.1$ Hz, $J = 3.4$ Hz), 7.46 (m, 2H), 7.83 (d, 2H, $J = 8.8$ Hz), 12.40 (s, 1H). MS, m/z (rel. intensity): 209 (100.0, M), 118 (7.6, M – 91).

To obtain **6**, 15 mmol of 1,2-benzenediamine (Aldrich) were added to a stirred solution of 15 mmol of 4-dimethylaminobenzoic acid (Aldrich) in 25 mL of toluene at 90 °C. 18 mmol of PCl₃ were then added dropwise and the mixture was kept refluxing for 12 h. The solid obtained was repeatedly washed with toluene and the product recrystallized from ethanol. ¹H NMR (300 MHz, DMSO), δ (ppm): 3.05 (s, 6H), 6.90 (d, 2H, $J = 8.7$ Hz), 7.35 (dd, 2H, $J = 3.1$ Hz, $J = 5.9$ Hz), 7.64 (dd, 2H, $J = 3.1$ Hz, $J = 5.9$ Hz), 8.06 (d, 2H, $J = 8.7$ Hz). MS, m/z (rel. intensity): 237 (100.0, M), 222 (9.2, M – 15), 194 (9.2, M – 43), 119 (11.3, M – 118).

2.2. Methods. Solutions were made up in double-distilled water and spectroscopy-grade solvents, and were not degassed. Acidity was varied with HClO₄ in non-aqueous solutions, and with HClO₄, NaOH or NaH₂PO₄ / Na₂HPO₄ buffer (all Merck p.a. products) in aqueous solutions. Non-aqueous solutions were either slightly acidified or strongly acidified to have the compounds in the ground state as the monocations or the dications, respectively, as confirmed by UV-vis absorption spectroscopy and comparison with the well-known spectra of the cations in

1
2
3 aqueous solutions. Sample concentrations of $\sim 10^{-5}$ mol dm⁻³ for absorption and $\sim 10^{-6}$ mol dm⁻³
4
5 for fluorescence were employed. All experiments were carried out at 25 °C.
6
7

8 pH was measured with a Radiometer PHM 82 pH meter equipped with a Radiometer Type B
9
10 combined electrode. Reported pK_a are practical values obtained from pH measurements and
11
12 concentrations of acid and base, measured from the absorption spectra. They are not corrected to
13
14 obtain the true thermodynamic values.
15
16

17 UV-vis absorption spectra were recorded in a Varian Cary 3E spectrophotometer.
18
19 Fluorescence excitation and emission spectra were recorded in a Spex Fluorolog-2 FL340 E1 T1
20
21 spectrofluorometer, with correction for instrumental factors by means of a Rhodamine B
22
23 quantum counter and correction files supplied by the manufacturer. Fluorescence quantum yields
24
25 were measured using quinine sulfate ($< 3 \times 10^{-5}$ mol dm⁻³) in aqueous H₂SO₄ (0.5 mol dm⁻³) as
26
27 standard ($\phi = 0.546$).^{50,51} The estimated standard uncertainty of the fluorescence quantum yields
28
29 measurements was 5 %. Fluorescence lifetimes were determined by single-photon timing in an
30
31 Edinburgh Instruments FL-900 spectrometer equipped with a hydrogen-filled nanosecond
32
33 flashlamp and the reconvolution analysis software supplied by the manufacturer.
34
35
36
37
38

39 Model equations were fitted to the experimental data by means of a non-linear weighted least-
40
41 squares routine based on the Marquardt algorithm. The reported uncertainties represent the
42
43 statistical standard deviations obtained in the fits.
44
45
46

47 3. RESULTS

48
49
50
51 **3.1. Absorption Spectra of 1, 2, 3, 2-OMe, and 3-OMe in Aqueous Solutions.** The
52
53 absorption spectra of **1** in aqueous solutions under neutral and acidic conditions are shown in
54
55 Figure 1a. The absorption spectrum of **1** in neutral medium showed an intense band at 31000
56
57
58
59
60

1
2
3 cm^{-1} and a weaker band at $\sim 27000 \text{ cm}^{-1}$. On decreasing the pH from neutral solution, the
4
5
6
7
8
9
10
11
12
13
14
15
16
17
18
19
20
21
22
23
24
25
26
27
28
29
30
31
32
33
34
35
36
37
38
39
40
41
42
43
44
45
46
47
48
49
50
51
52
53
54
55
56
57
58
59
60

cm^{-1} and a weaker band at $\sim 27000 \text{ cm}^{-1}$. On decreasing the pH from neutral solution, the absorption spectrum shifted to the red and its molar absorption coefficient increased with respect to that observed under neutral conditions. A new spectrum, peaking at 29320 cm^{-1} , was observed at pH 3.02. A further decrease of pH strongly shifted the absorption spectrum to the blue, the molar absorption coefficient decreasing to less than half its value at pH ~ 3 . The absorbance-pH data of **1** at 35710 cm^{-1} and at 27780 cm^{-1} are given in the inset of Figure 1a.

The absorption spectra obtained for **2** and the methoxy derivative **2-OMe** in aqueous solutions at different acidities (Figure 1, parts b and c) showed the same general features as those of **1**. The absorption spectrum recorded for **2-OMe** at pH ~ 10 showed however only one band similar in shape and position to the intense absorption band obtained for **1** and **2** under neutral conditions. The absorbance-pH curves were similar for **1**, **2**, and **2-OMe** (insets of Figure 1).

The absorption spectra of **3** and the methoxy derivative **3-OMe** in aqueous solutions at different acidities are shown in Figure 2. The absorption spectrum of **3** under neutral conditions, peaking at 30500 cm^{-1} , was very broad (Figure 2a). Upon acidifying the solution (pH ~ 5), the spectrum shifted to the red (maximum at 28740 cm^{-1}) and the molar absorption coefficient significantly increased. A further increase of acidity strongly shifted the spectrum to the blue, and a new band, peaking at 35460 cm^{-1} , was obtained at $[\text{HClO}_4] \sim 0.7 \text{ mol dm}^{-3}$, its maximum molar absorption coefficient decreasing to about half the value obtained for the absorption spectrum recorded at pH ~ 5 . Furthermore, increasing the pH from neutral conditions caused a blue shift of the spectrum, a new band being obtained at pH > 10 (results not shown). On the other hand, the absorption spectrum recorded for **3-OMe** in aqueous solutions under strongly ($[\text{HClO}_4] = 0.1 \text{ mol dm}^{-3}$) and mildly (pH ~ 5) acidic conditions were very similar to those obtained for **3**. Upon increasing the pH from pH 5, the absorption spectrum of **3-OMe** strongly

1
2
3 shifted to the blue, and a new band (peaking at 32150 cm^{-1}) was obtained at $\text{pH} > 8$, this
4
5 absorption spectrum being $\sim 1600\text{ cm}^{-1}$ blue shifted with respect to that measured for **3** at
6
7 $\text{pH} \sim 8$. The insets of Figures 2a and 2b show the absorbance-pH data for compounds **3** and
8
9 **3-OMe**.
10
11

12
13 **3.2. Fluorescence Spectra, Quantum Yields, and Lifetimes of 1, 2, 3, 2-OMe, 3-OMe, 5,**
14
15 **and 6 in Various Solvents under Strongly Acidic Conditions (Ground-State Diprotonated**
16
17 **Species).** The fluorescence spectra of **1, 2, 2-OMe, 3,** and **3-OMe** in strongly acidified aqueous
18
19 solution and acetonitrile (where the ground-state species are the dications **DC**, see later) are
20
21 shown in Figure 3. The fluorescence spectra of **1, 2,** and **3** exhibited the same general features,
22
23 and the excitation spectra matched the first absorption band measured under the same conditions.
24
25 The emission spectra of **2** and **3** in water showed only one band (at about $22000\text{-}23000\text{ cm}^{-1}$),
26
27 strongly red shifted with respect to its excitation spectrum. However, for **1** the main emission
28
29 band (at 23000 cm^{-1}) was accompanied by a shoulder at about 27000 cm^{-1} , which overlapped its
30
31 excitation spectrum. In acidified acetonitrile, the emission spectra of **1, 2,** and **3**, located at about
32
33 27000 cm^{-1} , were very similar to those recorded for **2-OMe** and **3-OMe** in acidified aqueous
34
35 solution, except for a weak emission observed at $\sim 22000\text{ cm}^{-1}$, not detected for the methoxy
36
37 derivatives. The fluorescence quantum yields Φ_{DC} of the species studied in this work in different
38
39 strongly acidified solvents are given in Table 1.
40
41
42
43
44
45

46
47 The fluorescence of **2-OMe** exhibited monoexponential decays both in aqueous solution and
48
49 acetonitrile, with the same lifetime (1.7 ns, Table 2). A monoexponential decay was also
50
51 observed for **2** in aqueous solution at 23260 cm^{-1} , with a lifetime of 3.8 ns. In acetonitrile, the
52
53 fluorescence decay was monoexponential at the main emission band (in the range 24390 cm^{-1} to
54
55
56
57
58
59
60

1
2
3 28570 cm^{-1}) with a lifetime of 1.5 ns, and became biexponential at lower wavenumbers with
4
5 lifetimes of 1.5 ns and 4.0 ns (at 23260 cm^{-1} , see Table 2).
6
7

8 **3.3. Fluorescence Spectra, Quantum Yields, and Lifetimes of 1, 2, 3, 2-OMe, 3-OMe, 4, 5,**
9 **and 6 in Various Solvents under Mildly Acidic Conditions (Ground-State Monoprotonated**
10 **Species).** The fluorescence spectra of **1** in mildly acidified aqueous solution and acetonitrile
11 (where the ground-state species exist as monocations, see later) are shown in Figure 4a. The
12 excitation and emission spectra of **1** were independent of the monitoring wavenumbers both in
13 acidified aqueous solution and acetonitrile. The emission spectrum in aqueous solution of pH
14 3.71 showed only one band, located at 25220 cm^{-1} , which overlapped its excitation spectrum.
15 This spectrum, peaking at 28450 cm^{-1} , coincided with the absorption spectrum of **1** measured
16 under the same acidity conditions. The fluorescence excitation spectrum of **1** measured in
17 slightly acidified acetonitrile overlapped its emission band and the emission spectrum almost
18 matched that observed in acidic aqueous solution.
19
20
21
22
23
24
25
26
27
28
29
30
31
32
33

34 The fluorescence behavior observed for **2** (Figure 4b) was very similar to that of **1** (Figure
35 4a). The excitation and emission spectra of **2-OMe** in acidified water were also independent of
36 the monitoring wavenumbers, and, except for a small red shift, showed the same features as the
37 excitation and emission bands recorded for **2** in the same solvent (Figure 4b).
38
39
40
41
42

43 The fluorescence spectra of **3** and **3-OMe** in slightly acidified acetonitrile are shown in Figure
44 4c. For both compounds, the excitation spectrum virtually matched the absorption spectrum
45 measured under the same acidity conditions, and the emission spectrum overlapped its excitation
46 spectrum. The fluorescence emission bands of **3** and **3-OMe** were much broader than the
47 emission bands recorded for **1**, **2**, and **2-OMe** in the same solvent. The emission spectrum of
48
49
50
51
52
53
54
55
56
57
58
59
60

1
2
3 **3-OMe** in acidified glycerol was however narrower than those recorded for **3** and **3-OMe** in
4 acetonitrile (Figure 4c).
5
6

7
8 The absorption and fluorescence spectra of the model compounds **4**, **5**, and **6** in slightly
9 acidified acetonitrile (so as to have all these compounds as the monocations) are shown in Figure
10 4d. For all compounds, the excitation spectrum matches the first absorption band and the
11 emission spectrum overlaps its excitation spectrum. Also, a red shift of both the excitation and
12 emission spectrum is observed on going from **4** to **5** and from **5** to **6**.
13
14
15
16
17
18

19
20 The fluorescence quantum yields Φ_{MC} of the monocationic species studied in this work,
21 obtained in different mildly acidified solvents, are compiled in Table 1. It is observed that the
22 quantum yields of **1** were similar to those of the model compound HBI, without the amino group.
23 However, the values measured for **2** were in some cases lower than those found for **1** and HBI,
24 and the effect was clearly stronger for **2-OMe**. Furthermore, the quantum yields of **2** and **2-OMe**
25 markedly increased with the solvent viscosity (especially for **2-OMe**), and decreased as the
26 dielectric permittivity of the solvent increased. The fluorescence quantum yields of **3** and **3-OMe**
27 were generally lower than those measured for **2** and **2-OMe**. The fluorescence quantum yields of
28 the monocations of model compounds **4**, **5** and **6**, with no hydroxyl or methoxy groups,
29 decreased in the series $\mathbf{4} \geq \mathbf{5} \gg \mathbf{6}$, the values decreasing up to 58 times (in acetonitrile) on going
30 from **5** to **6**.
31
32
33
34
35
36
37
38
39
40
41
42
43
44
45

46 Table 3 shows the fluorescence decays of **1**, **2**, **2-OMe**, **3-OMe**, and the model compounds **5**
47 and **6**, recorded in slightly acidified acetonitrile and 1-octanol. In acetonitrile, the decay was
48 monoexponential for **1** and **5** (lifetimes around 1.3 ns), but it became biexponential for the other
49 derivatives (lifetimes around 1 ns and 0.1 ns). The intensity fraction corresponding to the short
50 lifetime increased as the emission wavenumber decreased. For **3-OMe**, the biexponential decay
51
52
53
54
55
56
57
58
59
60

1
2
3 obtained at 23530 cm^{-1} with lifetimes of 1.9 ns (5 %) and 0.216 ns (95 %) became
4
5 monoexponential at 21740 cm^{-1} with a lifetime of 0.164 ns. In slightly acidified 1-octanol, the
6
7 fluorescence decay of **2** became monoexponential (lifetime 1.28 ns), whereas **2-OMe**, **3-OMe**,
8
9 and **6** exhibited biexponential decays (Table 3), with a long lifetime around 1 ns and a shorter
10
11 one in the range 0.3 ns to 0.6 ns.
12
13

14 15 16 **4. DISCUSSION**

17
18
19
20 **4.1. Ground-State Acid–Base Equilibria of 1, 2, 3, 2-OMe, and 3-OMe in Aqueous**
21
22 **Solution: First Protonation Occurs at the Benzimidazole Nitrogen.** In a previous paper, we
23
24 showed that **1**, **2**, and **3** in neutral aqueous solution exhibit tautomeric equilibria between the
25
26 normal form **N** and the tautomer **T** (see Chart 1), the last species being responsible for the red-
27
28 shifted absorption band appearing at $\sim 27000\text{ cm}^{-1}$.⁴¹ This equilibrium is impossible for **2-OMe**
29
30 and **3-OMe**, which exist only as normal form **N** and lack this absorption band.
31
32

33
34 The absorption spectra of **1**, **2**, and **2-OMe** (Figure 1), as well as those of **3** and **3-OMe**
35
36 (Figure 2) in aqueous solutions at different acidities indicate the existence of two acid-base
37
38 equilibria for all these compounds in the pH ranges studied. A global analysis of the
39
40 absorbance-pH data at different fixed wavenumbers was performed for each of the compounds
41
42 investigated (insets of Figures 1 and 2), yielding the pK_a values listed in Table 4. We include also
43
44 in this Table the pK_a values obtained by the same method for **4**, **5**, and **6**, some of which were
45
46 already measured by other authors.^{52,53} Our results indicate that the species involved in the
47
48 ground-state acid-base equilibria for all compounds with an amino group in neutral-to-acid
49
50 media are: the neutral form, the monocation **MC**, and the dication **DC** (see Scheme 1, where for
51
52 **1**, **2**, and **3**, species **T** in equilibrium with **N** has been omitted for clarity). Protonation of the
53
54
55
56
57
58
59
60

1
2
3 neutral form to give the monocation can take place at the benzimidazole N3 or at the amino N. In
4
5 agreement with previous studies on **6**,⁵² we propose that the first protonation occurs for all the
6
7 species at the benzimidazole N3, based on the following facts:
8
9

10 (1) The absorption spectra of the neutral form and the monocation of **1** and **2** were red shifted
11
12 (stronger for **2** than for **1**) with respect to those of HBI (Figures 5a and 5b) and showed a higher
13
14 molar absorption coefficient (Figure 1) than the neutral form and the monocation of HBI.³⁴ This
15
16 reveals a more extended π -electron conjugation for the neutral and monoprotonated forms of **1**
17
18 and **2** than for those of HBI, which must be due to the involvement of the nitrogen lone pair at
19
20 the $-\text{NH}_2$ or $-\text{NEt}_2$ group in the resonance system. The stronger electron-donating ability of
21
22 diethylaniline ($E_{\text{ox}} = 0.34 \text{ V}$)⁵⁴ compared to that of aniline ($E_{\text{ox}} = 0.54 \text{ V}$)⁵⁴ causes a more
23
24 extended π -conjugation in **2** than in **1**. As the absorption spectra of the monocations of **2-OMe**,
25
26 **3**, and **3-OMe** were very similar to those of **1** and **2** (Figures 1 and 2), we propose that the
27
28 neutral form of all these species protonates also at the benzimidazole N3.
29
30
31
32
33

34 (2) The absorption spectra of the dications of **1** and **2**, for which the amino group is
35
36 protonated (and therefore unable to act as an electron donor), coincided in shape and position
37
38 with the absorption spectrum of the monocation of HBI (Figure 5c), suggesting a similar
39
40 structure for the species involved.
41
42
43

44 (3) For both **1** and **2**, the molar absorption coefficients of the monocations were about 1.5
45
46 times higher than those of the neutral forms. In contrast, no difference was observed for HBI.³⁴
47
48 This must be due to the presence in the monocations of **1** and **2** of a positively charged
49
50 benzimidazolium ring (better electron acceptor than the benzimidazole moiety of the neutral
51
52 form), its charge withdrawing ability increasing the electron conjugation with the aminophenyl
53
54 group.
55
56
57
58
59
60

1
2
3 The involvement of the amino nitrogen lone pair in the π system is also responsible for the
4 differences between the pK_a values of HBI and those of its amino derivatives. It is observed in
5
6 Table 4 that the pK_{a2} value increased in the order $\text{HBI} < \mathbf{1} < \mathbf{2}$. This is explained by the fact that
7
8 the amino group at C4' causes an increase of the electron density (and therefore the basicity) at
9
10 the benzimidazole N3, stronger for $-\text{NEt}_2$ than for $-\text{NH}_2$. The same effect explains the pK_a
11
12 increase for monocation deprotonation in the series $\mathbf{4} < \mathbf{5} < \mathbf{6}$ (Table 4). Besides, it is also
13
14 observed that the pK_a value corresponding to protonation of the amino group was more than 2
15
16 units lower for $\mathbf{1}$ and $\mathbf{2}$ (pK_{a1}) than for aniline (pK_{a2} in Table 4). This must be due to the fact that
17
18 the electron density at the amino N is much higher for aniline than for protonated $\mathbf{1}$ and $\mathbf{2}$, as the
19
20 electron density is displaced toward the protonated benzimidazole ring.
21
22
23
24
25
26

27 The basicity at benzimidazole N3 increases with OH substitution at C2', as shows the pK_a
28
29 increase on going from $\mathbf{4}$ to HBI and from $\mathbf{5}$ to $\mathbf{1}$ (pK_{a2} in Table 4). This effect is stronger for the
30
31 methoxy group, as evidenced by the higher pK_{a2} values for the methoxy derivatives $\mathbf{2-OMe}$ and
32
33 $\mathbf{3-OMe}$ than for the hydroxy compounds $\mathbf{2}$ and $\mathbf{3}$ (Table 4). These results indicate that the OH
34
35 and OMe groups at the ortho position of the phenyl ring increase the electron density at the
36
37 benzimidazole N, this effect being stronger for OMe than for OH.
38
39
40

41 The experimental pK_a values allow us to arrange the substituent groups of the phenyl moiety
42
43 according to their electron-donor capacity to the benzimidazole unit. This is depicted in Chart 2,
44
45 together with the relative steric interactions of the aromatic rings.
46
47

48 **4.2. Excited-State Behavior of $\mathbf{1}$, $\mathbf{2}$, $\mathbf{3}$, $\mathbf{2-OMe}$, and $\mathbf{3-OMe}$ in Strongly Acidic Solutions:**
49
50 **Photodissociation of the Dication DC^* at the Hydroxyl Group.** The fluorescence excitation
51
52 spectrum of $\mathbf{1}$, $\mathbf{2}$, and $\mathbf{3}$ in strongly acidic aqueous solution and acetonitrile (Figure 3) can be
53
54 attributed to the dication DC , as it matched for each compound the absorption spectrum of DC
55
56
57
58
59
60

1
2
3 recorded in the same acidity conditions. Likewise, the fluorescence excitation spectrum of
4 **2-OMe** and **3-OMe** in strongly acidic aqueous solution (Figures 3b and 3c) is attributed to the
5 dication, as it is very similar to the absorption band of **DC** in the same solvent (Figures 1c and
6 2b). The absorption and fluorescence excitation spectra shown in Figure 3 reveal a great
7 similarity of the spectra for **1**, **2**, and **2-OMe**, and a blue shift of the spectra for **3** and **3-OMe**
8 with respect to those of the other compounds. This behavior can be explained by assuming that
9 the methyl group at benzimidazole N1 in **3** and **3-OMe** greatly enhances the steric hindrance
10 between adjacent ring systems, causing the dications of **3** and **3-OMe** to be nonplanar, **DC_{np}**.
11 The loss of conjugation in **DC_{np}** would result in a blue shift of its absorption and excitation
12 spectrum with respect to the planar form **DC** of **1**, **2**, and **2-OMe**, and a change in the shape of
13 the spectrum. Similar results were obtained for other methylated benzimidazole derivatives.^{55,56}
14
15
16
17
18
19
20
21
22
23
24
25
26
27
28

29 The fluorescence spectra in strongly acidified solutions shown in Figure 3 reveal a similar
30 behavior for **1**, **2**, and **3** in acetonitrile, and for **2-OMe** and **3-OMe** in water, only a greater
31 Stokes shift being detected for **3** and **3-OMe**. A completely different emission spectrum is
32 nevertheless observed for **1**, **2**, and **3** in water, which will be discussed later.
33
34
35
36
37
38

39 Under excitation of **DC** in acetonitrile for **1** and **2**, and in water for **2-OMe**, a single emission
40 band overlapping its excitation spectrum was observed (Figure 3), which we assign to **DC***. For
41 the dications of **3** in acetonitrile, and **3-OMe** in water, the emission spectrum was located in the
42 same position as that detected for the dications of **1**, **2**, and **2-OMe**, showing only some loss of
43 structure. This result contrasts with the absorption and excitation spectra, which were clearly
44 blue shifted for **3** and **3-OMe**, as discussed above. This causes that for **3** and **3-OMe** the
45 emission spectrum of the dication hardly overlaps its excitation band, and the Stokes shift is very
46 large. This indicates a great structural change from the ground to the excited state for **3** and
47
48
49
50
51
52
53
54
55
56
57
58
59
60

1
2
3 **3-OMe** dication. As the emission spectrum for these compounds appears in the same position as
4 those of the planar dications of **1**, **2**, and **2-OMe**, we propose that the ground-state nonplanar
5 dication DC_{np} of **3** and **3-OMe** reaches a planar conformation in the excited state from which
6 fluorescence takes place. Similar behavior was found for related systems.^{55,56}
7
8
9

10
11
12 The fluorescence quantum yields of the dications of **1**, **2**, **3**, **2-OMe**, and **3-OMe** (Table 1)
13 were high and showed only a weak dependence on the solvent properties. Similar results were
14 obtained for the model compounds **5** and **6** (Table 1).
15
16
17

18
19
20 Very different fluorescence behavior was observed for **1**, **2**, and **3** on changing the solvent
21 from strongly acidified acetonitrile to water. In aqueous solution, excitation of the dication led to
22 a red-shifted emission spectrum, with maximum at 22000-23000 cm^{-1} and very large Stokes shift
23 (Figure 3). This indicates that the initially excited dication is converted in the excited state to
24 another species, whose fluorescence is detected. This excited-state transformation does not take
25 place for the dications of the methoxy derivatives **2-OMe**, and **3-OMe** (Figures 3b and 3c).
26
27
28
29
30
31
32
33

34 It is well known that many phenol derivatives are stronger acids in the excited state. The
35 acidity increase upon excitation is even stronger for cationic species like the monocations of
36 HBI,³⁴ 2-(3'-hydroxy-2'-pyridyl)benzimidazole,⁴⁸ and 2-(1'-hydroxy-2'-
37 naphthyl)benzimidazole,^{19,49} protonated at the benzimidazole N3. These species behave as strong
38 photoacids, which deprotonate upon excitation at the hydroxyl group, totally in water and very
39 efficiently in alcohols. We propose that the dications of **1**, **2**, and **3** are also strong photoacids
40 that transfer their hydroxyl proton to water upon excitation to yield the fluorescent tautomeric
41 monocation TC^* , protonated at the benzimidazole N3 and at the amino group, and deprotonated
42 at the hydroxyl group (Scheme 2). This species is a tautomer of the monocation MC present in
43 the ground state. As the spectrum of the red-shifted emission of TC^* is similar for **1**, **2**, and **3**,
44
45
46
47
48
49
50
51
52
53
54
55
56
57
58
59
60

1
2
3 we assume that TC^* has the same planar structure for all three species. This implies that
4
5 excitation of the nonplanar dication of **3**, DC_{np} , is followed by deprotonation and rotational
6
7 relaxation in the excited state to yield the planar TC^* form with intramolecular hydrogen bond
8
9 $\text{O}^{\cdot}\cdots\text{H}-\text{N}$ (Scheme 3).
10
11

12
13 The dication of **1** seems to be a weaker photoacid than those of **2** and **3**, as the red-shifted
14
15 emission of TC^* is accompanied by a weak shoulder at emission wavenumbers corresponding to
16
17 the undissociated dication (Figure 3a). This shoulder is not detected in the fluorescence spectra
18
19 of **2** and **3**.
20
21

22
23 The emission spectrum of **1**, **2**, and **3** in acidified acetonitrile shows a shoulder at lower
24
25 wavenumbers that is not detected for **2-OMe** and **3-OMe** and is located at the same position as
26
27 the emission maximum of TC^* in water. We suggest that this weak emission corresponds to a
28
29 small amount of TC^* formed in acetonitrile, this process being favored by minor amounts of
30
31 water in this solvent.
32
33

34
35 Fluorescence decay measurements performed for **2** and **2-OMe** (Table 2) in strongly acidified
36
37 solvents support the previous assignments. As expected, the fluorescence decay was
38
39 monoexponential for **2-OMe**. The same lifetime (1.7 ns) is obtained in acetonitrile and in water,
40
41 which is assigned to **2-OMe** DC^* . The monoexponential decay obtained for **2** in strongly
42
43 acidified aqueous solution led to a lifetime value of 3.8 ns, which is assigned to the species TC^*
44
45 formed by dissociation of the excited dication. Monoexponential decay was also obtained for **2**
46
47 in acetonitrile at higher emission wavenumbers, with a lifetime of 1.55 ns attributed to DC^* .
48
49 This value is similar to that of **2-OMe** DC^* (1.7 ns). Biexponential decay was detected for **2** in
50
51 acetonitrile in the lower-wavenumber region. The second lifetime (4.05 ns) was very similar to
52
53 the fluorescence lifetime of TC^* in water (3.8 ns). This result confirms the assignment of the
54
55
56
57
58
59
60

1
2
3 lower-wavenumber shoulder in the emission spectrum of **2** in acetonitrile (Figure 3b) to the
4
5 fluorescence of **TC***.
6
7

8
9
10 **4.3. Excited-State Behavior of 1, 2, 3, 2-OMe, 3-OMe, 4, 5, and 6 in Mildly Acidic**
11 **Solutions: Deactivation of the Monocation MC* by Intramolecular Charge Transfer.** For
12
13 both **1** and **2** in slightly acidic aqueous solution, the fluorescence excitation spectrum matched
14
15 the absorption spectrum recorded in the same conditions (Figures 4a and 4b), and therefore it
16
17 must be due to the main species present at this acidity, the monocation **MC** protonated at the
18
19 benzimidazole N3 (Scheme 1). This means that excitation of **MC** originates the one-band
20
21 emission spectrum, which was independent of the excitation wavenumber, and overlapped its
22
23 excitation spectrum. These results indicate that **MC*** is the fluorescent species. The fluorescence
24
25 excitation and emission spectra of **1** and **2** in slightly acidified acetonitrile were practically
26
27 coincident with the spectra measured in water, and the spectra of **2-OMe** were very similar to
28
29 that of **2** (Figures 4a and 4b). These results led us to conclude that for **1**, **2**, and **2-OMe** in
30
31 slightly acidified acetonitrile and water, the monocation **MC** is the only absorbing and
32
33 fluorescent species.
34
35
36
37
38
39

40
41 The above results indicate that the monocations of **1** and **2** do not dissociate in the excited
42
43 state in water. This behavior is clearly different from that showed by the monocations of the
44
45 related compounds HBI,³⁴ 2-(3'-hydroxy-2'-pyridyl)benzimidazole,⁴⁸ and 2-(1'-hydroxy-2'-
46
47 naphthyl)benzimidazole.^{19,49} For all these compounds, the excited monocation is a strong
48
49 photoacid, that deprotonates at the hydroxyl group to yield the neutral tautomer **T***, totally in
50
51 water and very efficiently in short-chain alcohols. The fact that the monocations of **1** and **2** do
52
53 not deprotonate in the excited state must be related to the presence in these compounds of a -NH₂
54
55
56
57
58
59
60

1
2
3 or a $-\text{NEt}_2$ group. The charge donation of these groups to the phenol ring must inhibit
4 dissociation at the hydroxyl group, as consequence of the increase in the excited-state $\text{p}K_a$ value
5 of the OH group of **1** and **2** with respect to those of HBI and related compounds lacking the
6 amino group.
7
8
9
10

11
12 The absorption and fluorescence spectra of **3** and **3-OMe** in acidified acetonitrile (Figure 4c)
13 showed the same general features as those of **1**, **2**, and **2-OMe** (Figures 4a and 4b). The
14 excitation spectrum matched the absorption spectrum of **MC**, and the emission spectrum
15 overlapped its excitation spectrum. This indicates that the emission band of **3** and **3-OMe** is also
16 due to **MC***. However, it is seen that the emission spectra of **3** and **3-OMe** were much broader
17 than those recorded for **1**, **2** and **2-OMe** (Figures 4a, 4b, and 4c). This suggests that the
18 fluorescence of **MC*** is accompanied by the emission of a second species for **3** and **3-OMe**. The
19 identity of this species will be discussed later.
20
21
22
23
24
25
26
27
28
29
30

31
32 In spite of the similarity between the fluorescence spectrum of monoprotonated **1**, **2**, and
33 **2-OMe**, a close look at the fluorescence quantum yields (Φ_{MC} , Table 1) and lifetimes values (τ_1
34 and τ_2 , Table 3) reveals important differences between **1** and its derivatives **2** and **2-OMe**. It is
35 observed in Table 1 that both HBI and its amino derivative **1** showed monocation fluorescence
36 quantum yields in the range 0.24 to 0.36 in all the solvents studied (except **1** in water, $\Phi_{\text{MC}} =$
37 0.10). However, Φ_{MC} values for **2** and **2-OMe** (with a $-\text{NEt}_2$ group at C4') were lower than for **1**
38 and HBI in solvents of high polarity or/and low viscosity, this effect being stronger for the
39 methylated derivative **2-OMe**.
40
41
42
43
44
45
46
47
48
49
50

51
52 The fluorescence quantum yields of **3** monocation were lower than that of **2** (Table 1), and the
53 same occurs for **3-OMe** and **2-OMe**. As can be seen in Table 1, Φ_{MC} values were relatively high
54 for **3-OMe** in very viscous solvents (1-octanol, glycerol...), but they decreased as solvent
55
56
57
58
59
60

1
2
3 viscosity decreased and/or solvent polarity increased, showing the same behavior as **2** and
4
5 **2-OMe**.

6
7
8 To investigate the effect of the hydroxyl or methoxy groups of **1**, **2**, **3**, and derivatives on their
9
10 fluorescence behavior, we studied the model compounds **4**, **5**, and **6**, with no hydroxyl or
11
12 methoxy substituents at C4' (Chart 2). The absorption and fluorescence spectra as well as the
13
14 pK_a values of these compounds in aqueous solution have already been reported.^{52,53,57} It has been
15
16 shown that the first protonation of **4**, **5**, and **6** takes place, like for HBI and its amino and
17
18 diethylamino derivatives, at the benzimidazole N3 to give monocation **MC**. For **4**, **5**, and **6**, the
19
20 absorption spectrum of **MC** in acidified acetonitrile and the excitation and emission spectra in
21
22 the same solvent are shown in Figure 4d. We conclude from these spectra that for the three
23
24 compounds excitation of **MC** leads to **MC*** fluorescence. However, whereas **MC*** fluorescence
25
26 quantum yields were high for **4** and **5** (Table 1), and virtually independent of solvent (as for HBI
27
28 and **1**), for **6** the values drastically decreased with respect to those of **4** and **5**. Moreover, Φ_{MC}
29
30 values for **6** strongly decreased as the solvent polarity increased and solvent viscosity decreased.
31
32
33
34
35

36
37 The above results provide compelling evidence that the monocations of **6**, **2**, **2-OMe**, **3**, and
38
39 **3-OMe** undergo in the excited state a radiationless deactivation process which increases its
40
41 efficiency as the solvent polarity increases and the solvent viscosity decreases. Moreover, the
42
43 strong dependence of the process with the solvent viscosity suggests that it involves a large-
44
45 amplitude motion. Also, as neither the monocations of HBI and **1**, nor those of **4** and **5**
46
47 experience that radiationless deactivation, we conclude that the presence of the -NEt₂ or -NMe₂
48
49 substituent at C4' strongly favors the occurrence of the process. To explain these results, we
50
51 propose that the radiationless deactivation undergone by the monocations of **2**, **2-OMe**, **3**,
52
53 **3-OMe**, and **6** is an intramolecular charge migration, from the diethyl- or dimethylaminophenyl
54
55
56
57
58
59
60

1
2
3 ring (donor) to the protonated benzimidazole moiety (acceptor), connected to a large-amplitude
4 rotational motion (TICT process), to give a non-fluorescent charge-transfer intermediate MC_{ct}^*
5
6 (Scheme 4). Moreover, as species **1** does not undergo that process, we can conclude that the
7
8 aminohydroxyphenyl ring is not a good enough electron donor. An analogous charge-transfer
9
10 process has been previously reported by us⁴¹ for the neutral tautomer T^* of compounds **2** and **3**
11
12 from the deprotonated diethylaminophenol ring to the protonated benzimidazole to give a non-
13
14 fluorescent charge-transfer intermediate. A similar polarity- and viscosity-dependent
15
16 photoinduced intramolecular charge transfer coupled to an interannular torsional motion has
17
18 been proposed for related systems, as for example hydroxyphenylbenzoxazole
19
20 and -benzothiazole,⁴⁵ [(dimethylamino)phenyl]methylpyridinium,⁵⁸ phenol-pyridinium cation,⁵⁹
21
22 and hydroxyphenylimidazopyridines.^{60,61} Different theoretical and experimental approaches have
23
24 been used to elucidate the nature of the intramolecular charge transfer processes in these and
25
26 other donor-acceptor organic molecules.^{40,62-66}
27
28
29
30
31
32
33

34 Taking into account that the charge-transfer process undergone by MC^* involves a
35
36 conformational motion, we would expect the process to be more efficient for **3** and **3-OMe** than
37
38 for **2** and **2-OMe**, because the steric hindrance of the methyl group at benzimidazole N1 in **3** and
39
40 **3-OMe** would facilitate the conformational motion needed for the process to take place. A close
41
42 look at the data in Table 1 reveals that, as expected, Φ_{MC} values were lower for **3** and **3-OMe**
43
44 than for **2** and **2-OMe**. However, the emission spectrum of MC^* in acetonitrile was for **3** and
45
46 **3-OMe** much broader than that recorded for the monocations of **1**, **2**, and **2-OMe** (Figure 4), but
47
48 it became narrower in very viscous solvents like glycerol (Figure 4c). This suggests that, for the
49
50 N-methyl derivatives, the charge-transfer species might be fluorescent, leading to a broad
51
52 emission spectrum, comprising the fluorescence of MC^* and MC_{ct}^* . However, in very viscous
53
54
55
56
57
58
59
60

1
2
3 solvents, like glycerol, where conformational motion cannot take place, and therefore the process
4
5 $\text{MC}^* \rightarrow \text{MC}_{\text{ct}}^*$ is inhibited, emission is virtually due only to MC^* . Emission from an
6
7 intramolecular charge-transfer state has been reported for the related compounds
8
9 dimethylaminophenylimidazopyridines,⁶⁷⁻⁶⁹ and also for the well-known
10
11 dimethylaminobenzonitrile and related species.⁷⁰
12
13

14
15 Additionally, it is observed in Table 1 that Φ_{MC} values were clearly lower for **2-OMe** than for
16
17 **2**. This is also in agreement with our interpretation of the results, because the methoxy group in
18
19 **2-OMe** slightly improves the strength of the electron donor, and therefore the charge-transfer
20
21 efficiency is higher for **2-OMe** than for **2**. As deduced from the values in Table 1, this effect is
22
23 not significant for **3-OMe**, with quantum yields similar to **3**, probably due to the fact that the
24
25 steric hindrance of the methyl group at benzimidazole N1 in both compounds strongly facilitates
26
27 the torsional motion connected to the charge transfer.
28
29
30

31
32 From the proposed mechanism (Scheme 4), monoexponential fluorescence decays would be
33
34 expected for the monocations of the investigated compounds. However, fluorescence decays
35
36 were biexponential for all the compounds except **1** and **5**, and **2** in 1-octanol (see Table 3). For **2**,
37
38 **2-OMe**, **3-OMe**, and **6** in acetonitrile, the value of lifetime τ_1 (~1.1 ns) was very similar to that
39
40 obtained for **1** and **5** (~1.3 ns), which do not experience the intramolecular charge-transfer
41
42 process $\text{MC}^* \rightarrow \text{MC}_{\text{ct}}^*$, and its contribution increased with the emission wavenumber. Lifetime τ_2
43
44 (the shorter times are at the resolution limit of our equipment) tends to be shorter, and its
45
46 intensity fraction higher, for compounds with lower Φ_{MC} values, indicating its relation to the
47
48 process $\text{MC}^* \rightarrow \text{MC}_{\text{ct}}^*$. In the more viscous solvent 1-octanol, the process $\text{MC}^* \rightarrow \text{MC}_{\text{ct}}^*$, should
49
50 be less efficient than in acetonitrile. In agreement with this, τ_2 values (Table 3) significantly
51
52 increased on going from acetonitrile to 1-octanol for **2**, **2-OMe**, **3-OMe**, and **6**, and its intensity
53
54
55
56
57
58
59
60

1
2
3 fraction significantly decreased. For **2**, the fluorescence decay in 1-octanol was monoexponential
4
5 with a τ_1 value (1.28 ns) very similar to that of **1** and **5** in acetonitrile, indicating that the charge
6
7 transfer process is not efficient for **2** in this solvent.
8
9

10 A possible explanation for this behavior is that **MC*** emission takes place from different
11 multistep-relaxation structures. Under this assumption, the observed biexponential fluorescence
12 decay would be a simplification of a non-exponential decay. The complex decay kinetics
13 observed for the monocations here studied has also been found for other charge-transfer
14 molecular rotors, as for example p-(9-anthryl)-N,N-dimethylaniline,⁷¹ auramine^{72,73} and
15 Thioflavin-T.⁷⁴ Non-exponential and wavelength-dependent kinetics is a common characteristic
16 for this type of molecules, and several theoretical models were proposed to explain the complex
17 decay.⁷¹⁻⁷⁴
18
19
20
21
22
23
24
25
26
27
28
29

30 5. CONCLUSIONS

31
32 We have shown that the first protonation of compounds **1**, **2**, **3**, **2-OMe**, and **3-OMe** in the
33 ground state takes place at the benzimidazole N3 to give monocation **MC**. The second
34 protonation occurs at the amino group to yield dication **DC** (nonplanar for **3** and **3-OMe**). In
35 acetonitrile, under excitation of **DC**, fluorescence from **DC*** was observed for all these
36 compounds. In aqueous solution, the excited dication **DC*** of **1**, **2**, and **3** behaves as a strong
37 photoacid, deprotonating (totally for **2** and **3**) at the hydroxyl group to yield the fluorescent
38 tautomeric monocation **TC***. This species, protonated at the imidazole and amino nitrogens, and
39 deprotonated at the hydroxyl group, does not exist in significant amounts in the ground state.
40 After deactivation, **TC** protonates again to regenerate **DC**.
41
42
43
44
45
46
47
48
49
50
51
52
53
54

55 Unlike HBI and some derivatives, the excited monocations of **1**, **2**, and **3** did not deprotonate
56 at the hydroxyl group and fluorescence from **MC*** was detected for **1**, **2**, **3**, and their methoxy
57
58
59
60

1
2
3 derivatives in all the solvents investigated. On the other hand, whereas the monocation
4
5 fluorescence quantum yield of **1** was virtually independent of solvent, those of **2**, **3**, **2-OMe**,
6
7
8 **3-OMe** and the simple model compound **6** showed a viscosity- and polarity-dependent
9
10 radiationless deactivation associated to a large-amplitude conformational motion undergone by
11
12 **MC***. We have shown that this rotational motion is connected to an intramolecular charge
13
14 transfer (TICT) from the phenyl unit to the protonated benzimidazole moiety, to give a charge-
15
16 transfer structure **MC_{ct}***. Fluorescence from this charge-transfer species could only be detected
17
18 for **3** and **3-OMe**. The efficiency of this process, not observed for **1**, **4**, and **5**, increased with the
19
20 strength of the electron-donor group and with the steric hindrance of the methyl group at
21
22 benzimidazole N1.
23
24
25
26
27
28
29
30
31
32
33
34
35
36
37
38
39
40
41
42
43
44
45
46
47
48
49
50
51
52
53
54
55
56
57
58
59
60

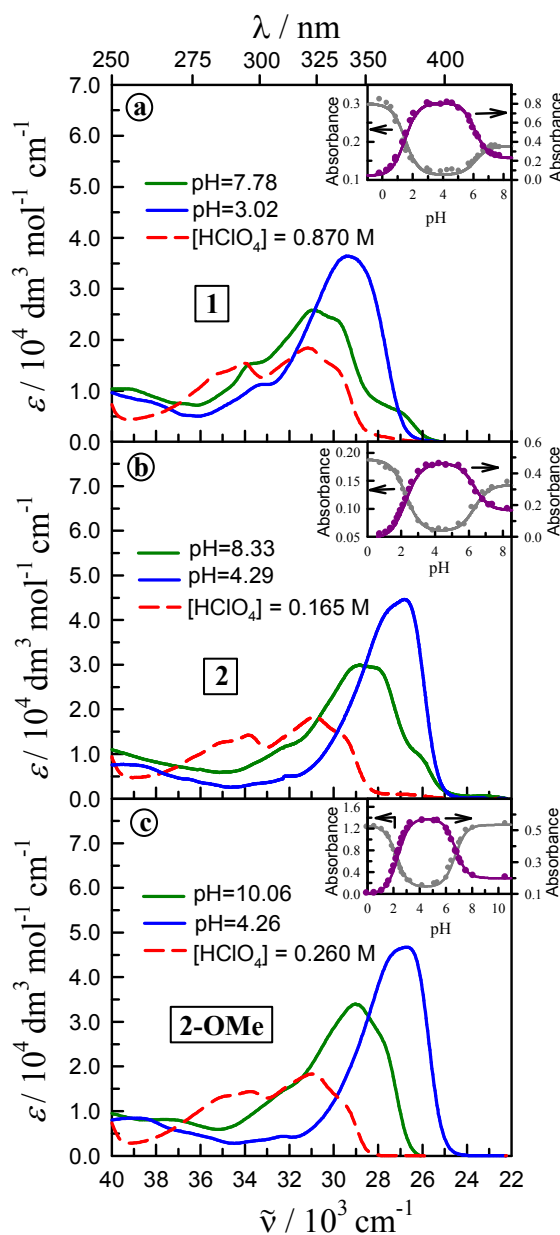


Figure 1. Absorption spectra of (a) **1**, (b) **2**, and (c) **2-OMe** in neutral, mildly acidic and strongly acidic aqueous solution. The insets show the pH dependence of the absorbance in aqueous solution (a) for **1** at 27780 cm^{-1} (●) and at 35710 cm^{-1} (●); (b) for **2** at 27030 cm^{-1} (●) and at 31250 cm^{-1} (●); and (c) for **2-OMe** at 27030 cm^{-1} (●) and at 31250 cm^{-1} (●).

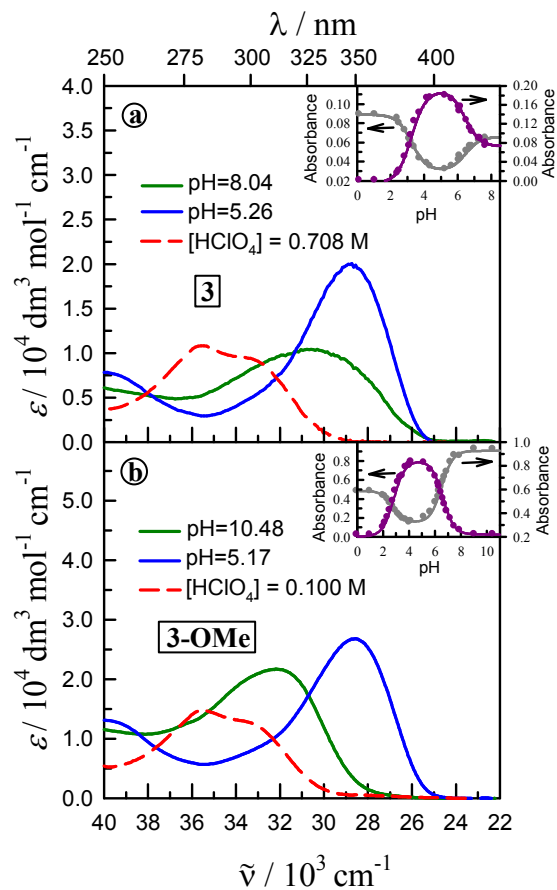


Figure 2. Absorption spectra of (a) **3** and (b) **3-OMe** in neutral, mildly acidic and strongly acidic aqueous solution. The insets show the pH dependence of the absorbance (a) for **3** at 28570 cm^{-1} (\bullet) and at 34480 cm^{-1} (\bullet), and (b) for **3-OMe** at 27030 cm^{-1} (\bullet) and at 33330 cm^{-1} (\bullet).

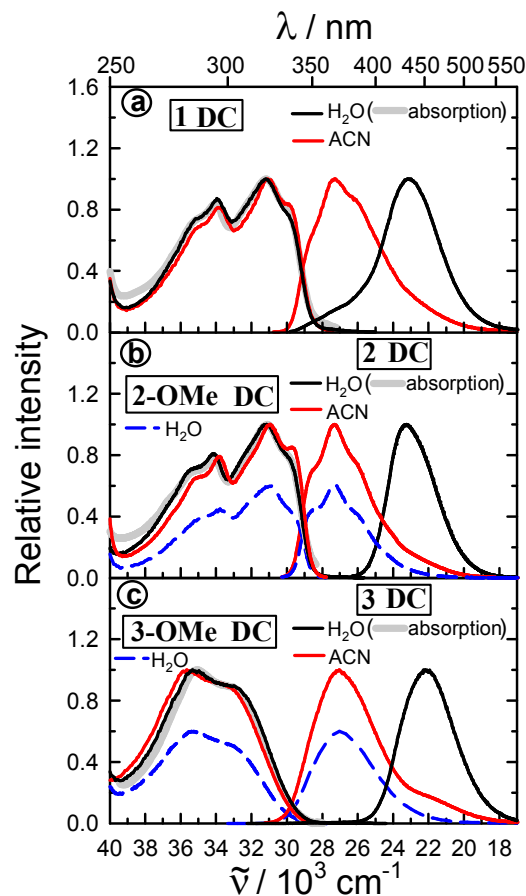


Figure 3. Normalized fluorescence excitation and emission spectra in strongly acidified solutions of (a) **1** in acetonitrile ($\tilde{\nu}_{exc} = 31060 \text{ cm}^{-1}$, $\tilde{\nu}_{em} = 27250 \text{ cm}^{-1}$) and water ($\tilde{\nu}_{exc} = 31150 \text{ cm}^{-1}$, $\tilde{\nu}_{em} = 22990 \text{ cm}^{-1}$), (b) **2** in acetonitrile ($\tilde{\nu}_{exc} = 30770 \text{ cm}^{-1}$, $\tilde{\nu}_{em} = 27400 \text{ cm}^{-1}$) and water ($\tilde{\nu}_{exc} = 30770 \text{ cm}^{-1}$, $\tilde{\nu}_{em} = 23260 \text{ cm}^{-1}$), and **2-OMe** in water ($\tilde{\nu}_{exc} = 30860 \text{ cm}^{-1}$, $\tilde{\nu}_{em} = 27170 \text{ cm}^{-1}$), and (c) **3** in acetonitrile ($\tilde{\nu}_{exc} = 35650 \text{ cm}^{-1}$, $\tilde{\nu}_{em} = 27030 \text{ cm}^{-1}$) and water ($\tilde{\nu}_{exc} = 35340 \text{ cm}^{-1}$, $\tilde{\nu}_{em} = 22200 \text{ cm}^{-1}$) and **3-OMe** in water ($\tilde{\nu}_{exc} = 35460 \text{ cm}^{-1}$, $\tilde{\nu}_{em} = 27030 \text{ cm}^{-1}$). The absorption spectra of **1**, **2**, and **3** in aqueous solution of the same pH as that of the fluorescence spectra are also shown (—).

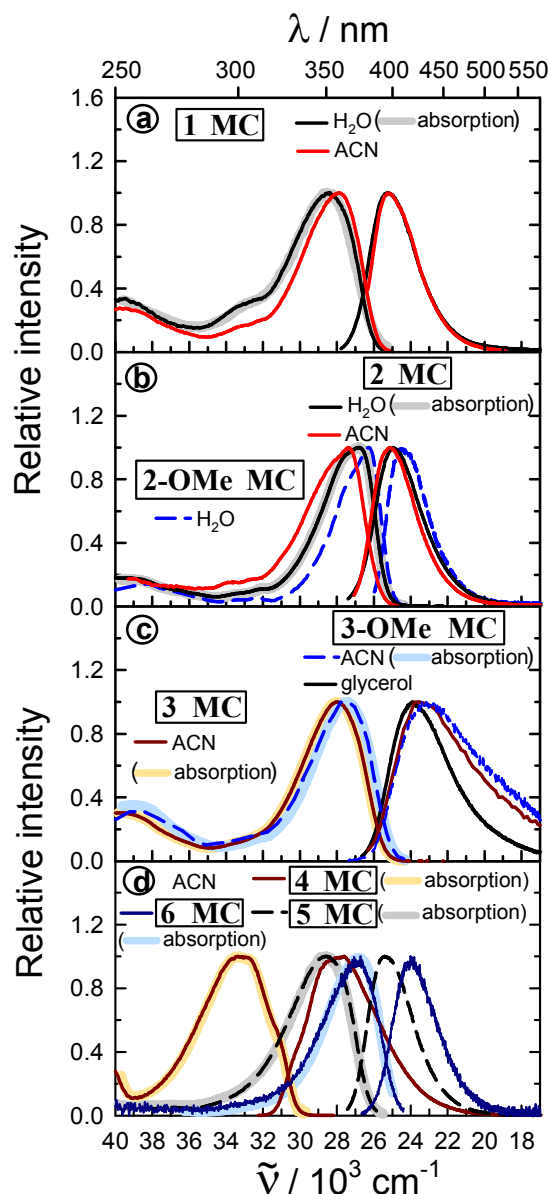


Figure 4. Absorption spectra and normalized fluorescence excitation and emission spectra of the monoprotonated forms of the indicated species in mildly acidic solutions. (a) **1** in acetonitrile ($\tilde{\nu}_{exc} = 27930 \text{ cm}^{-1}$, $\tilde{\nu}_{em} = 25190 \text{ cm}^{-1}$) and water at pH 3.71 ($\tilde{\nu}_{exc} = 28410 \text{ cm}^{-1}$, $\tilde{\nu}_{em} = 25190 \text{ cm}^{-1}$), (b) **2** in acetonitrile ($\tilde{\nu}_{exc} = 27400 \text{ cm}^{-1}$, $\tilde{\nu}_{em} = 25160 \text{ cm}^{-1}$) and water at pH 4.71 ($\tilde{\nu}_{exc} = 26820 \text{ cm}^{-1}$, $\tilde{\nu}_{em} = 24970 \text{ cm}^{-1}$) and **2-OMe** in acetonitrile ($\tilde{\nu}_{exc} = 26320 \text{ cm}^{-1}$, $\tilde{\nu}_{em} = 24440 \text{ cm}^{-1}$), (c) **3** in acetonitrile ($\tilde{\nu}_{exc} = 28010 \text{ cm}^{-1}$, $\tilde{\nu}_{em} = 23530 \text{ cm}^{-1}$) and **3-OMe** in acetonitrile ($\tilde{\nu}_{exc} = 28010 \text{ cm}^{-1}$, $\tilde{\nu}_{em} = 23150 \text{ cm}^{-1}$) and glycerol ($\tilde{\nu}_{exc} = 23920 \text{ cm}^{-1}$), and (d) **4** ($\tilde{\nu}_{exc} = 33330 \text{ cm}^{-1}$, $\tilde{\nu}_{em} = 27620 \text{ cm}^{-1}$), **5** ($\tilde{\nu}_{exc} = 28570 \text{ cm}^{-1}$, $\tilde{\nu}_{em} = 25380 \text{ cm}^{-1}$), and **6** ($\tilde{\nu}_{exc} = 26740 \text{ cm}^{-1}$, $\tilde{\nu}_{em} = 24040 \text{ cm}^{-1}$) in acetonitrile.

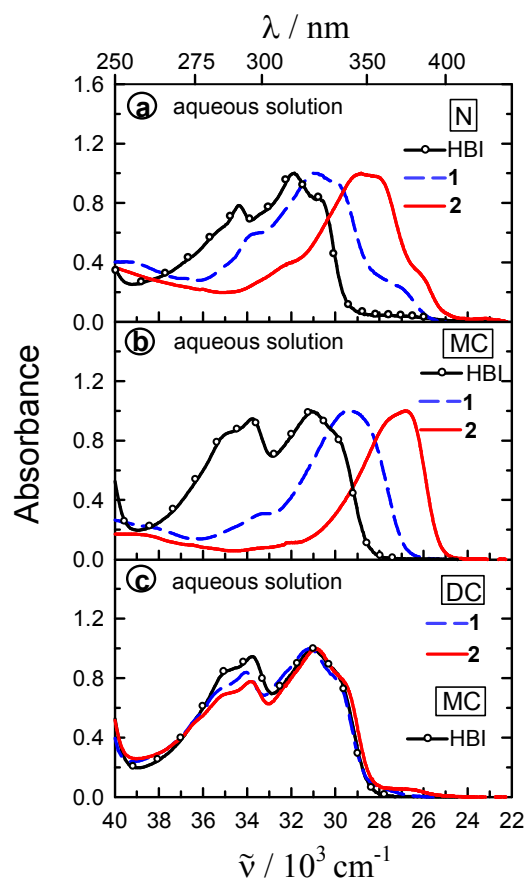


Figure 5. Normalized absorption spectra in aqueous solution of (a) the neutral forms and (b) the monocations of HBI, **1**, and **2**. In part (c), the spectra of the dications of **1** and **2** are compared with that of the monocation of HBI.

Chart 1. Molecular Structures of the Neutral Isomers of HBI, 1, 2, and 3. The Normal Forms (N_{syn} , N_{anti} , N_{np}) and the Tautomer T Obtained after ESIPT Are Shown

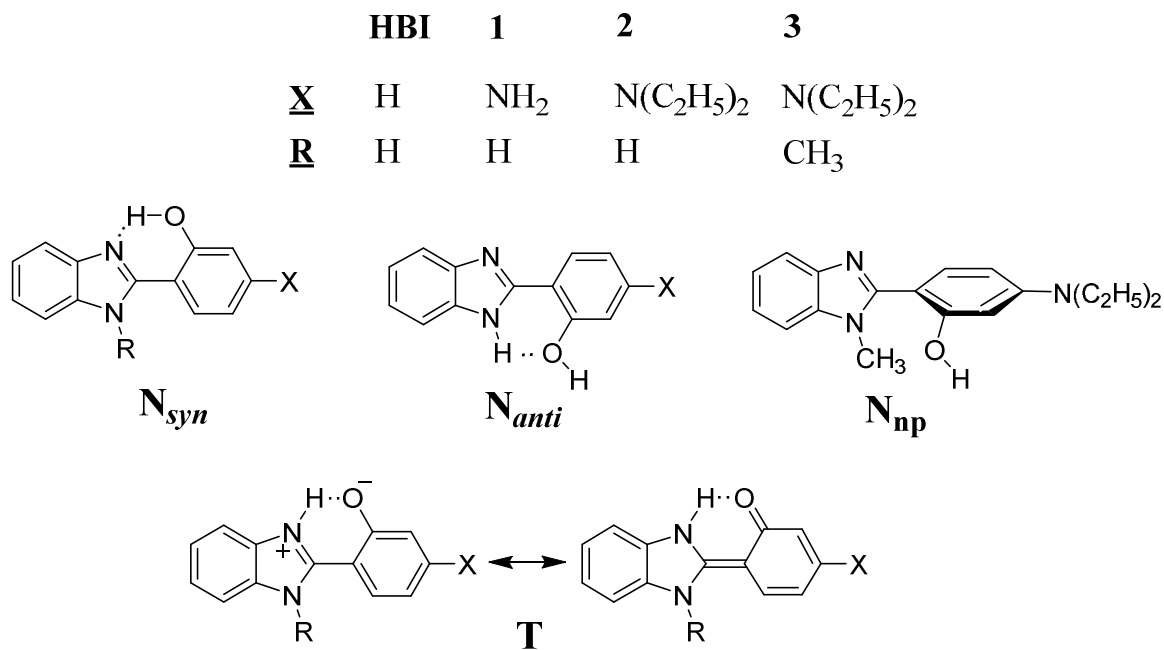
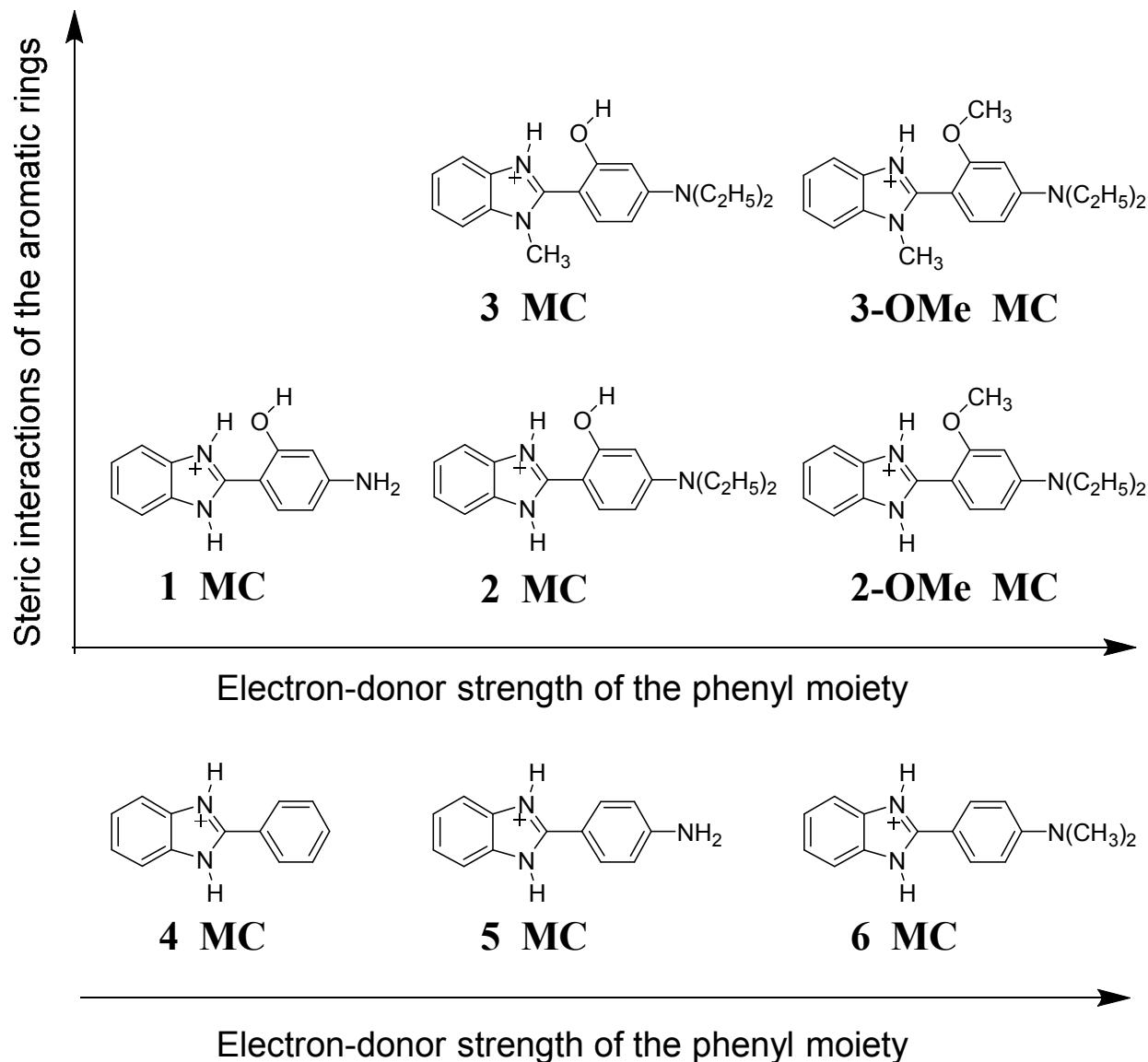
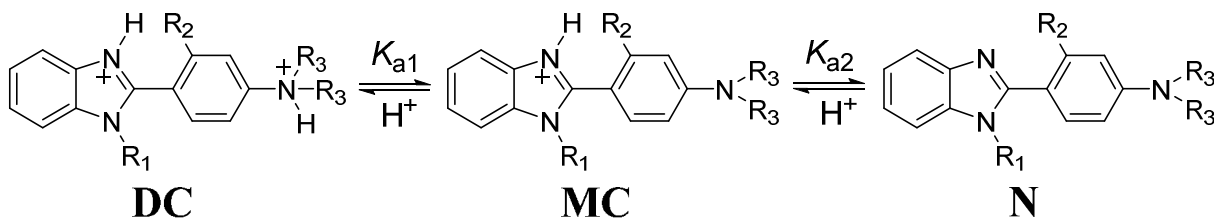


Chart 2. Molecular Structures of the Monocations (MC) Studied in this Work, Ordered as Function of the Electron-Donor Strength of the Phenyl Moiety and the Steric Interactions of the Aromatic Rings



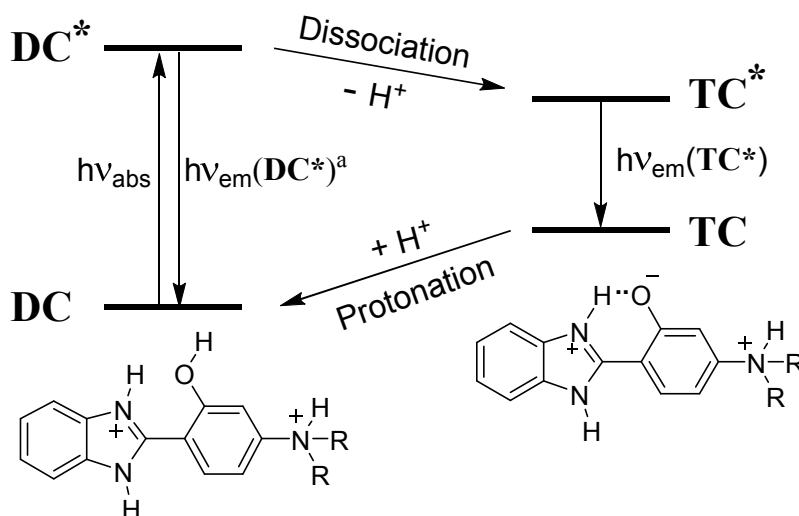
Scheme 1. Acid–Base Equilibria of **1**, **2**, **2-OMe**, **3**, **3-OMe**, **5** and **6** ($R_1 = \text{H}$ or CH_3 , $R_2 = \text{H}$, OH , or OCH_3 , $R_3 = \text{H}$, CH_3 , or C_2H_5), showing the dication (**DC**),^a the monocation (**MC**) and the neutral form (**N**)^b



^a For **3** and **3-OMe**, **DC** has a nonplanar structure.

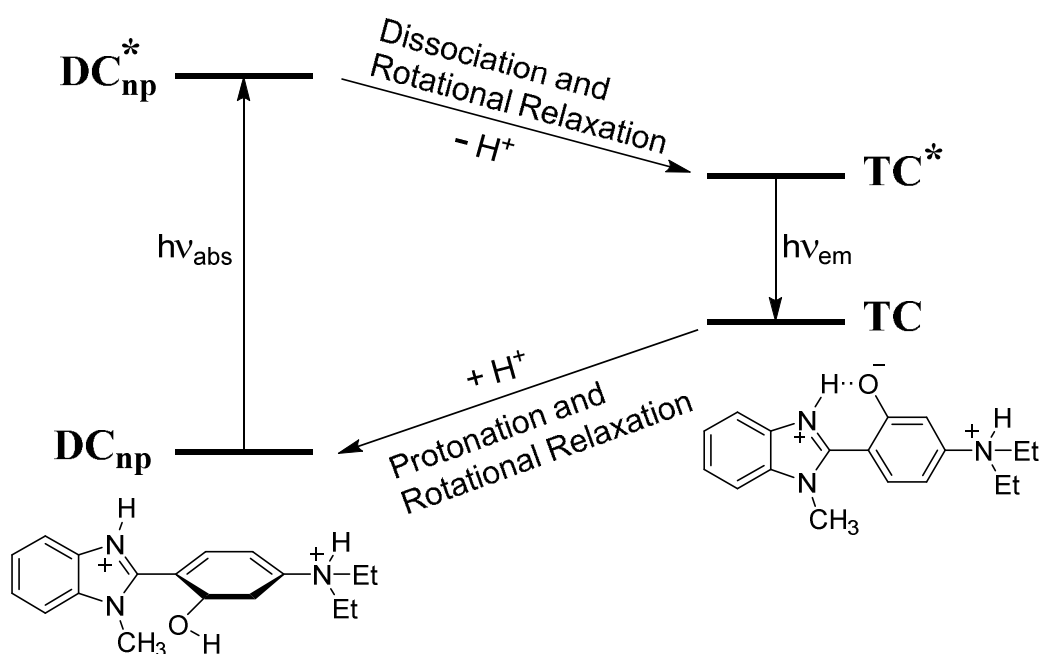
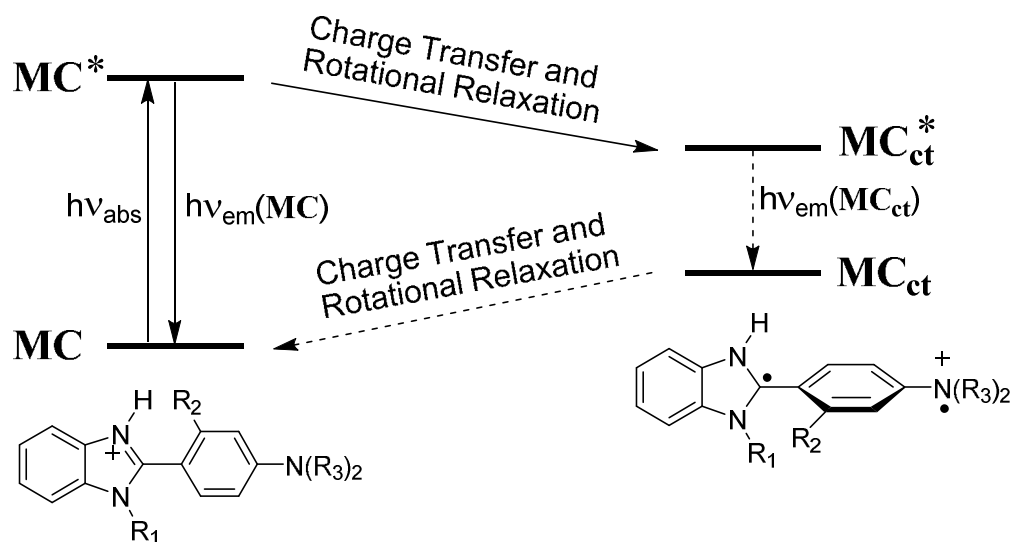
^b For **1**, **2**, and **3**, the neutral tautomer **T** exist in equilibrium with **N** in neutral aqueous solution. **N** has nonplanar structure for **3** and **3-OMe** in aqueous solution (see ref. ⁴¹).

Scheme 2. Excitation and Deactivation Pathways of the Dications of **1** and **2** in Aqueous Solution



^a Fluorescence of **DC*** in water detected only for **1**.

Scheme 3. Excitation and Deactivation Pathways of the Dication of 3 in Aqueous Solution

Scheme 4. Excitation and Deactivation Pathways of the Monocation of Compounds 6, 2, 2-OMe, 3, and 3-OMe^a

^a MC_{ct}^{*} fluoresces slightly for 3 and 3-OMe.

Table 1. Fluorescence Quantum Yields of the Species Studied in this Work at 298 K in Various Mildly (Φ_{MC} , Monocations) and Strongly Acidified (Φ_{DC} , Dications) Solvents for Which the Viscosity and the Relative Dielectric Permittivity Are Shown

Solvent	ϵ_r^a	η^b/cP	Φ_{MC}									Φ_{DC}							
			4	5	6	HBI	1	2	2-OMe	3	3-OMe	5	6	1	2	2-OMe	3	3-OMe	
dioxane	2.21	1.44	0.35	0.28	0.10			0.19	0.14							0.42	0.38		
diethyl ether	4.20	0.24		0.30	0.27								0.42						
ethyl acetate	6.02	0.45			0.09	0.36		0.21	0.14				0.27	0.37	0.55				
tetrahydrofuran	7.58	0.55		0.48	0.09	0.26	0.24	0.27	0.09		0.07		0.13		0.38			0.26	
acetonitrile	35.94	0.36	0.47	0.41	0.007	0.32	0.24	0.07	0.01	0.01	0.01	0.54	0.42	0.23	0.50	0.60	0.14		
N,N-dimethylformamide	36.71	0.92		0.42	0.01														
dimethyl sulfoxide	46.45	1.99		0.47	0.015		0.24	0.12	0.02		0.01								
1-octanol	10.30	10.64			0.21		0.27	0.37	0.27		0.16		0.25		0.43		0.24		
2-butanol	16.56	4.21			0.12		0.33	0.49	0.21				0.23		0.43				
ethanol	24.55	1.20	0.47	0.52	0.03		0.25	0.26	0.06	0.02	0.03		0.28		0.46		0.26		
methanol	32.66	0.55			0.01		0.29	0.14	0.03				0.18		0.46				
water	78.30	1.00	0.42	0.11	0.005		0.10	0.02	0.008			0.32	0.39		0.41				
ethylene glycol	37.70	19.90			0.06			0.15	0.07				0.21		0.40				
glycerol	42.50	1412			0.15			0.32	0.26		0.14		0.19						

^a Values at 298.15 K from ref. ⁷⁵. ^b Values at 298.15 K from ref. ⁷⁶.

Table 2. Fluorescence Lifetimes τ_1 and τ_2 and Associated Fractional Intensities (in Square Brackets) of 2 and 2-OMe in Acetonitrile and Water under Excitation of Dication DC in Strongly Acidic Conditions at 298 K. The Species to which each Lifetime Was Assigned Are Also Shown.

Compound	$\tilde{\nu}_{\text{exc}}/\text{cm}^{-1}$	$\tilde{\nu}_{\text{em}}/\text{cm}^{-1}$	τ_1/ns	τ_2/ns	χ^2
Strongly acidified acetonitrile					
2 DC	30770	28570	1.522 ± 0.005 (DC*)		1.038
	30770	24390	1.587 ± 0.005 (DC*)		1.153
	30770	23260	1.5 ^a [52 %] (DC*)	4.05 ± 0.04 [48 %] (TC*)	1.092
2-OMe DC	31250	27030	1.744 ± 0.003 (DC*)		1.018
	31250	23810	1.755 ± 0.003 (DC*)		1.124
Strongly acidified aqueous solution					
2 DC	30770	23260	3.812 ± 0.002 (TC*)		1.072
2-OMe DC	33330	25974	1.679 ± 0.004 (DC*)		1.022
	33330	24390	1.714 ± 0.004 (DC*)		1.092

^a Fixed value, obtained at emission wavenumbers where the decay is monoexponential. Fixing this value, a more precise value of τ_2 is obtained at this wavenumber.

Table 3. Fluorescence Lifetimes τ_1 and τ_2 and Associated Fractional Intensities (in Parenthesis) of the Indicated Species in Slightly Acidified Acetonitrile and 1-Octanol under Excitation of Monocation MC at 298 K

Compound	$\tilde{\nu}_{\text{exc}}/\text{cm}^{-1}$	$\tilde{\nu}_{\text{em}}/\text{cm}^{-1}$	τ_1/ns	τ_2/ns	χ^2
Slightly acidified acetonitrile					
1 MC	27030	24390	1.340 ± 0.007		1.088
2 MC	26320	25000	1.125 ± 0.008 (74 %)	0.22 ± 0.02 (26 %)	1.052
	26320	24390	1.112 ± 0.007 (72 %)	0.15 ± 0.02 (28 %)	1.055
	26320	23260	1.148 ± 0.008 (66 %)	0.17 ± 0.01 (34 %)	1.084
2-OMe MC	26320	25320	1.16 ± 0.04 (10 %)	0.124 ± 0.006 (90 %)	1.003
	26320	24690	1.18 ± 0.04 (6 %)	0.121 ± 0.005 (94 %)	1.019
	26320	23810	1.13 ± 0.04 (5 %)	0.092 ± 0.004 (95 %)	1.128
3-OMe MC	28170	23530	1.9 ± 0.1 (5 %)	0.216 ± 0.008 (95 %)	1.018
	28170	21740		0.164 ± 0.007	1.009
5 MC	27030	25000	1.264 ± 0.002		1.009
6 MC	26320	25000	0.9 ± 0.1 (29 %) ^a	0.08 ± 0.01 (71 %) ^a	1.041
	26320	23810	0.9 ± 0.1 (13 %) ^a	0.08 ± 0.01 (87 %) ^a	1.072
Slightly acidified 1-octanol					
2 MC	25970	24390	1.275 ± 0.003		1.024
	25970	22220	1.294 ± 0.003		1.123
2-OMe MC	25640	24100	1.078 ± 0.006 (86 %)	0.31 ± 0.03 (14 %)	1.001
	25640	22730	1.098 ± 0.008 (83 %)	0.37 ± 0.04 (17 %)	1.084
3-OMe MC	27780	25320	1.20 ± 0.01 (55 %)	0.47 ± 0.02 (45 %)	1.040
	27780	22220	1.22 ± 0.01 (78 %)	0.54 ± 0.05 (22 %)	1.186
6 MC	26320	25000	1.1 ± 0.1 (51 %) ^a	0.6 ± 0.1 (49 %) ^a	1.185
	26320	23810	1.1 ± 0.1 (44 %) ^a	0.6 ± 0.1 (56 %) ^a	1.022
	26320	22470	1.1 ± 0.1 (45 %) ^a	0.6 ± 0.1 (55 %) ^a	1.039

^a Global fit.

Table 4. Acidity Constants Obtained for the Compounds Studied in this Work and Some Simple Model Compounds in Aqueous Solution at 298 K

Compound	pK_{a1}	pK_{a2}
	DC \rightleftharpoons MC	MC \rightleftharpoons N
1	1.50 \pm 0.01	6.11 \pm 0.02
2	2.29 \pm 0.01	6.31 \pm 0.02
2-OMe	2.34 \pm 0.02	6.74 \pm 0.02
3	3.25 \pm 0.01	6.44 \pm 0.03
3-OMe	2.85 \pm 0.06	6.60 \pm 0.01
HBI		5.48 \pm 0.09 ^a
4		4.95 \pm 0.05
5	1.48 \pm 0.01	5.95 \pm 0.02
6	1.50 \pm 0.01	6.11 \pm 0.02
benzimidazole		5.53 ^b
aniline		4.63 ^c
<i>N,N</i> -diethylaniline		5.15 ^c

^a Value from ref. ³⁴. ^b Value from ref. ⁷⁷. ^c Values from ref. ⁷⁶.

AUTHOR INFORMATION

Corresponding Authors

*E-mail: carmen.rios@usc.es, manuel.mosquera@usc.es, flor.rodriiguez.prieto@usc.es

ACKNOWLEDGEMENTS

We are indebted to the European Regional Development Fund, the Spanish Ministry of Economy and Competitiveness (Grant CTQ2010-17835), and the Xunta de Galicia (Grants GPC2013/052, CN2012/314, and EM2012/091) for financial support of our work. S. R. and J. L. P. L. are thankful for a MEC-FPU fellowship and a “Ramón y Cajal” contract, respectively.

REFERENCES

- (1) Llano, J.; Eriksson, L. A. First Principles Electrochemical Study of Redox Events in DNA Bases and Chemical Repair in Aqueous Solution. *Phys. Chem. Chem. Phys.* **2004**, *6*, 2426-2433.
- (2) Borg, O. A.; Eriksson, L. A.; Durbeej, B. Electron-Transfer Induced Repair of 6-4 Photoproducts in DNA: A Computational Study. *J. Phys. Chem. A* **2007**, *111*, 2351-2361.
- (3) Sobolewski, A. L.; Domcke, W. Relevance of Electron-Driven Proton-Transfer Processes for the Photostability of Proteins. *ChemPhysChem* **2006**, *7*, 561-564.
- (4) Meyer, T. J.; Huynh, M. H. V.; Thorp, H. H. The Possible Role of Proton-Coupled Electron Transfer (PCET) in Water Oxidation by Photosystem II. *Angew. Chem., Int. Ed.* **2007**, *46*, 5284-5304.
- (5) Belevich, I.; Verkhovsky, M. I.; Wikstroem, M. Proton-Coupled Electron Transfer Drives the Proton Pump of Cytochrome c Oxidase. *Nature* **2006**, *440*, 829-832.
- (6) Weinberg, D. R.; Gagliardi, C. J.; Hull, J. F.; Murphy, C. F.; Kent, C. A.; Westlake, B. C.; Paul, A.; Ess, D. H.; McCafferty, D. G.; Meyer, T. J. Proton-Coupled Electron Transfer. *Chem. Rev.* **2012**, *112*, 4016-4093.
- (7) Chipem, F. A. S.; Mishra, A.; Krishnamoorthy, G. The Role of Hydrogen Bonding in Excited State Intramolecular Charge Transfer. *Phys. Chem. Chem. Phys.* **2012**, *14*, 8775-8790.
- (8) Demchenko, A. P.; Tang, K.-C.; Chou, P.-T. Excited-State Proton Coupled Charge Transfer Modulated by Molecular Structure and Media Polarization. *Chem. Soc. Rev.* **2013**, *42*, 1379-1408.
- (9) Hammes-Schiffer, S.; Soudackov, A. V. Proton-Coupled Electron Transfer in Solution, Proteins, and Electrochemistry. *J. Phys. Chem. B* **2008**, *112*, 14108-14123.
- (10) Ko, C.; Solis, B. H.; Soudackov, A. V.; Hammes-Schiffer, S. Photoinduced Proton-Coupled Electron Transfer of Hydrogen-Bonded p-Nitrophenylphenol-Methylamine Complex in Solution. *J. Phys. Chem. B* **2013**, *117*, 316-325.

- 1
2
3
4
5
6
7
8
9
10
11
12
13
14
15
16
17
18
19
20
21
22
23
24
25
26
27
28
29
30
31
32
33
34
35
36
37
38
39
40
41
42
43
44
45
46
47
48
49
50
51
52
53
54
55
56
57
58
59
60
- (11) Hsieh, C.-C.; Jiang, C.-M.; Chou, P.-T. Recent Experimental Advances on Excited-State Intramolecular Proton Coupled Electron Transfer Reaction. *Acc. Chem. Res.* **2010**, *43*, 1364-1374.
- (12) De Silva, A. P. Luminescent Photoinduced Electron Transfer (PET) Molecules for Sensing and Logic Operations. *J. Phys. Chem. Lett.* **2011**, *2*, 2865-2871.
- (13) Tian, H.; Yang, X.; Cong, J.; Chen, R.; Liu, J.; Hao, Y.; Hagfeldt, A.; Sun, L. Tuning of Phenoxazine Chromophores for Efficient Organic Dye-Sensitized Solar Cells. *Chem. Commun.* **2009**, 6288-6290.
- (14) Wu, Y.; Zhu, W. Organic Sensitizers from D- π -A to D-A- π -A: Effect of the Internal Electron-Withdrawing Units on Molecular Absorption, Energy Levels and Photovoltaic Performances. *Chem. Soc. Rev.* **2013**, *42*, 2039-2058.
- (15) Baranoff, E.; Barigelletti, F.; Bonnet, S.; Collin, J.-P.; Flamigni, L.; Mobian, P.; Sauvage, J.-P. From Photoinduced Charge Separation to Light-Driven Molecular Machines. *Struct. Bond.* **2007**, *123*, 41-78.
- (16) Agmon, N. Elementary Steps in Excited-State Proton Transfer. *J. Phys. Chem. A* **2005**, *109*, 13-35.
- (17) Pérez-Lustres, J. L.; Rodríguez-Prieto, F.; Mosquera, M.; Senyushkina, T. A.; Ernsting, N. P.; Kovalenko, S. A. Ultrafast Proton Transfer to Solvent: Molecularity and Intermediates from Solvation- and Diffusion-Controlled Regimes. *J. Am. Chem. Soc.* **2007**, *129*, 5408-5418.
- (18) Veiga-Gutiérrez, M.; Brenlla, A.; Carreira Blanco, C.; Fernández, B.; Kovalenko, S. A.; Rodríguez-Prieto, F.; Mosquera, M.; Pérez Lustres, J. L. Dissociation of a Strong Acid in Neat Solvents: Diffusion Is Observed after Reversible Proton Ejection Inside the Solvent Shell. *J. Phys. Chem. B* **2013**, *117*, 14065-14078.
- (19) Brenlla, A.; Veiga Gutiérrez, M.; Ríos Rodríguez, M. C.; Rodríguez-Prieto, F.; Mosquera, M.; Pérez Lustres, J. L. Moderately Strong Photoacid Dissociates in Alcohols with High Transient Concentration of the Proton-Transfer Contact Pair. *J. Phys. Chem. Lett.* **2014**, *5*, 989-994.
- (20) Mansueto, E. S.; Wight, C. A. Excited-State Proton-Transfer Polymerization of Amorphous Formaldehyde. *J. Am. Chem. Soc.* **1989**, *111*, 1900-1901.
- (21) Silvi, S.; Arduini, A.; Pochini, A.; Secchi, A.; Tomasulo, M.; Raymo, F. M.; Baroncini, M.; Credi, A. A Simple Molecular Machine Operated by Photoinduced Proton Transfer. *J. Am. Chem. Soc.* **2007**, *129*, 13378-13379.
- (22) Irie, M. Light-Induced Reversible pH Change. *J. Am. Chem. Soc.* **1983**, *105*, 2078-2079.
- (23) Paterson, M. J.; Robb, M. A.; Blancafort, L.; DeBellis, A. D. Mechanism of an Exceptional Class of Photostabilizers: A Seam of Conical Intersection Parallel to Excited State Intramolecular Proton Transfer (ESIPT) in o-Hydroxyphenyl-(1,3,5)-triazine. *J. Phys. Chem. A* **2005**, *109*, 7527-7537.
- (24) Sobolewski, A. L. Reversible Molecular Switch Driven by Excited-State Hydrogen Transfer. *Phys. Chem. Chem. Phys.* **2008**, *10*, 1243-1247.
- (25) Park, S.; Kwon, J. E.; Kim, S. H.; Seo, J.; Chung, K.; Park, S.-Y.; Jang, D.-J.; Medina, B. M.; Gierschner, J.; Park, S. Y. A White-Light-Emitting Molecule: Frustrated Energy Transfer between Constituent Emitting Centers. *J. Am. Chem. Soc.* **2009**, *131*, 14043-14049.
- (26) Formosinho, S. J.; Arnaut, L. G. Excited-State Proton Transfer Reactions. II. Intramolecular Reactions. *J. Photochem. Photobiol., A* **1993**, *75*, 21-48.
- (27) Ormson, S. M.; Brown, R. G. Excited State Intramolecular Proton Transfer part 1: ESIPT to Nitrogen. *Prog. React. Kinet.* **1994**, *19*, 45-91.

1
2
3 (28) Waluk, J.: *Conformational Analysis of Molecules in Excited States*; Wiley-VCH: New
4 York, 2000.

5
6 (29) Williams, D. L.; Heller, A. Intramolecular Proton Transfer Reactions in Excited
7 Fluorescent Compounds. *J. Phys. Chem.* **1970**, *74*, 4473-4480.

8 (30) Sinha, H. K.; Dogra, S. K. Ground- and Excited-State Prototropic Reactions in 2-(o-
9 Hydroxyphenyl)benzimidazole. *Chem. Phys.* **1986**, *102*, 337-347.

10 (31) Das, K.; Sarkar, N.; Majumdar, D.; Bhattacharyya, K. Excited-state Intramolecular
11 Proton Transfer and Rotamerism of 2-(2'-Hydroxyphenyl)benzimidazole. *Chem. Phys. Lett.*
12 **1992**, *198*, 443-448.

13 (32) Das, K.; Sarkar, N.; Ghosh, A. K.; Majumdar, D.; Nath, D. N.; Bhattacharyya, K.
14 Excited-State Intramolecular Proton Transfer in 2-(2-Hydroxyphenyl)benzimidazole and -
15 benzoxazole: Effect of Rotamerism and Hydrogen Bonding. *J. Phys. Chem.* **1994**, *98*, 9126-
16 9132.

17 (33) Douhal, A.; Amat-Guerri, F.; Lillo, M. P.; Acuna, A. U. Proton Transfer Spectroscopy of
18 2-(2'-Hydroxyphenyl)imidazole and 2-(2'-Hydroxyphenyl)benzimidazole Dyes. *J. Photochem.*
19 *Photobiol., A* **1994**, *78*, 127-138.

20 (34) Mosquera, M.; Penedo, J. C.; Ríos Rodríguez, M. C.; Rodríguez-Prieto, F. Photoinduced
21 Inter- and Intramolecular Proton Transfer in Aqueous and Ethanolic Solutions of 2-(2'-
22 Hydroxyphenyl)benzimidazole: Evidence for Tautomeric and Conformational Equilibria in the
23 Ground State. *J. Phys. Chem.* **1996**, *100*, 5398-5407.

24 (35) Ríos, M. A.; Ríos, M. C. Ab Initio Study of the Hydrogen Bond and Proton Transfer in 2-
25 (2'-Hydroxyphenyl)benzothiazole and 2-(2'-Hydroxyphenyl)benzimidazole. *J. Phys. Chem. A*
26 **1998**, *102*, 1560-1567.

27 (36) Tsai, H.-H. G.; Sun, H.-L. S.; Tan, C.-J. TD-DFT Study of the Excited-State Potential
28 Energy Surfaces of 2-(2'-Hydroxyphenyl)benzimidazole and its Amino Derivatives. *J. Phys.*
29 *Chem. A* **2010**, *114*, 4065-4079.

30 (37) Konoshima, H.; Nagao, S.; Kiyota, I.; Amimoto, K.; Yamamoto, N.; Sekine, M.; Nakata,
31 M.; Furukawa, K.; Sekiya, H. Excited-State Intramolecular Proton Transfer and Charge Transfer
32 in 2-(2'-Hydroxyphenyl)benzimidazole Crystals Studied by Polymorphs-Selected Electronic
33 Spectroscopy. *Phys. Chem. Chem. Phys.* **2012**, *14*, 16448-16457.

34 (38) Furukawa, K.; Yamamoto, N.; Nakabayashi, T.; Ohta, N.; Amimoto, K.; Sekiya, H.
35 Changes in the Electric Dipole Moments and Molecular Polarizabilities of Enol and Keto Forms
36 of 2-(2'-Hydroxyphenyl)benzimidazole Along the Proton Transfer Reaction Path in a PMMA
37 Film. *Chem. Phys. Lett.* **2012**, *539-540*, 45-49.

38 (39) Chipem, F. A. S.; Behera, S. K.; Krishnamoorthy, G. Enhancing Excited State
39 Intramolecular Proton Transfer in 2-(2'-Hydroxyphenyl)benzimidazole and Its Nitrogen-
40 Substituted Analogues by beta-Cyclodextrin: The Effect of Nitrogen Substitution. *J. Phys. Chem.*
41 *A* **2013**, *117*, 4084-4095.

42 (40) Chipem, F. A. S.; Krishnamoorthy, G. Comparative Theoretical Study of Rotamerism
43 and Excited State Intramolecular Proton Transfer of 2-(2'-Hydroxyphenyl)benzimidazole, 2-(2'-
44 Hydroxyphenyl)imidazo[4,5-b]pyridine, 2-(2'-Hydroxyphenyl)imidazo[4,5-c] pyridine and 8-(2'-
45 Hydroxyphenyl)purine. *J. Phys. Chem. A* **2009**, *113*, 12063-12070.

46 (41) Ríos Vázquez, S.; Ríos Rodríguez, M. C.; Mosquera, M.; Rodríguez-Prieto, F.
47 Rotamerism, Tautomerism, and Excited-State Intramolecular Proton Transfer in 2-(4'-N,N-
48 Diethylamino-2'-hydroxyphenyl)benzimidazoles: Novel Benzimidazoles Undergoing Excited-
49 State Intramolecular Coupled Proton and Charge Transfer. *J. Phys. Chem. A* **2008**, *112*, 376-387.

1
2
3 (42) Rodembusch, F. S.; Leusin, F. P.; Campo, L. F.; Stefani, V. Excited State Intramolecular
4 Proton Transfer in Amino 2-(2'-hydroxyphenyl)benzazole Derivatives: Effects of the Solvent and
5 the Amino Group Position. *J. Lumin.* **2007**, *126*, 728-734.

6
7 (43) Rodríguez Prieto, F.; Ríos Rodríguez, M. C.; Mosquera Gonzalez, M.; Ríos Fernandez,
8 M. A. Ground- and Excited-State Tautomerism in 2-(3'-Hydroxy-2'-pyridyl)benzimidazole. *J.*
9 *Phys. Chem.* **1994**, *98*, 8666-8672.

10 (44) Chipem, F. A. S.; Dash, N.; Krishnamoorthy, G. Role of Nitrogen Substitution in Phenyl
11 Ring on Excited State Intramolecular Proton Transfer and Rotamerism of 2-(2'-
12 Hydroxyphenyl)benzimidazole: A Theoretical Study. *J. Chem. Phys.* **2011**, *134*, 104308.

13 (45) Ríos Vázquez, S.; Ríos Rodríguez, M. C.; Mosquera, M.; Rodríguez-Prieto, F. Excited-
14 State Intramolecular Proton Transfer in 2-(3'-Hydroxy-2'-pyridyl)benzoxazole. Evidence of
15 Coupled Proton and Charge Transfer in the Excited State of Some o-Hydroxyarylbenzazoles. *J.*
16 *Phys. Chem. A* **2007**, *111*, 1814-1826.

17 (46) Levitt, J. A.; Kuimova, M. K.; Yahioğlu, G.; Chung, P.-H.; Suhling, K.; Phillips, D.
18 Membrane-Bound Molecular Rotors Measure Viscosity in Live Cells via Fluorescence Lifetime
19 Imaging. *J. Phys. Chem. C* **2009**, *113*, 11634-11642.

20 (47) Kuimova, M. K. Mapping Viscosity in Cells Using Molecular Rotors. *Phys. Chem.*
21 *Chem. Phys.* **2012**, *14*, 12671-12686.

22 (48) Mosquera, M.; Ríos Rodríguez, M. C.; Rodríguez-Prieto, F. Competition between
23 Protonation and Deprotonation in the First Excited Singlet State of 2-(3'-Hydroxy-2'-
24 pyridyl)benzimidazole in Acidic Solutions. *J. Phys. Chem. A* **1997**, *101*, 2766-2772.

25 (49) Brenlla, A.; Rodríguez-Prieto, F.; Mosquera, M.; Ríos, M. A.; Ríos Rodríguez, M. C.
26 Solvent-Modulated Ground-State Rotamerism and Tautomerism and Excited-State Proton-
27 Transfer Processes in o-Hydroxynaphthylbenzimidazoles. *J. Phys. Chem. A* **2009**, *113*, 56-67.

28 (50) Crosby, G. A.; Demas, J. N. Measurement of Photoluminescence Quantum Yields.
29 Review. *J. Phys. Chem.* **1971**, *75*, 991-1024.

30 (51) Melhuish, W. H. Quantum Efficiencies of Fluorescence of Organic Substances: Effect of
31 Solvent and Concentration of the Fluorescent Solute. *J. Phys. Chem.* **1961**, *65*, 229-235.

32 (52) Dey, J.; Dogra, S. K. Dual Fluorescence of 2-[4-(Dimethylamino)phenyl]benzothiazole
33 and Its Benzimidazole Analog: Effect of Solvent and pH on Electronic Spectra. *J. Phys. Chem.*
34 **1994**, *98*, 3638-3644.

35 (53) Mishra, A. K.; Dogra, S. K. Effect of Solvents and pH on the Absorption and
36 Fluorescence Spectra of 2-Phenylbenzimidazole. *Spectrochim. Acta*, **1983**, *39A*, 609-611.

37 (54) Weinberg, N. L.; Weinberg, H. R. Electrochemical Oxidation of Organic Compounds.
38 *Chem. Rev.* **1968**, *68*, 449-523.

39 (55) Ríos Rodríguez, M. C.; Rodríguez-Prieto, F.; Mosquera, M. Conformational Effects on
40 the Photoinduced Proton-Transfer Processes in 1-Methyl-2-(3'-hydroxy-2'-
41 pyridyl)benzimidazole. *Phys. Chem. Chem. Phys.* **1999**, *1*, 253-260.

42 (56) Rodríguez-Prieto, F.; Penedo, J. C.; Mosquera, M. Solvent Control of Molecular
43 Structure and Excited-State Proton-Transfer Processes of 1-Methyl-2-(2'-
44 hydroxyphenyl)benzimidazole. *J. Chem. Soc., Faraday Trans.* **1998**, *94*, 2775-2782.

45 (57) Mishra, A. K.; Dogra, S. K. Effects of Solvents and pH on the Spectral Behavior of 2-(p-
46 Aminophenyl)benzimidazole. *Bull. Chem. Soc. Jpn.* **1985**, *58*, 3587-3592.

47 (58) Fromherz, P.; Heilemann, A. Twisted Internal Charge-Transfer in
48 (Aminophenyl)pyridinium. *J. Phys. Chem.* **1992**, *96*, 6864-6866.

- 1
2
3 (59) Malval, J. P.; Chaumeil, H.; Rettig, W.; Kharlanov, V.; Diemer, V.; Ay, E.; Morlet-
4 Savary, F.; Poizat, O. Excited-State Dynamics of Phenol-Pyridinium Biaryl. *Phys. Chem. Chem.*
5 *Phys.* **2012**, *14*, 562-574.
- 6
7 (60) Brenlla, A.; Veiga, M.; Ríos Rodríguez, M. C.; Mosquera, M.; Rodríguez-Prieto, F.
8 Fluorescence of Methylated Derivatives of Hydroxyphenylimidazopyridine. Resolution of
9 Strongly Overlapping Spectra and a New ESIPT Dye Showing Very Efficient Radiationless
10 Deactivation. *Photochem. Photobiol. Sci.* **2011**, *10*, 1622-1636.
- 11 (61) Brenlla, A.; Veiga, M.; Pérez Lustres, J. L.; Ríos Rodríguez, M. C.; Rodríguez-Prieto, F.;
12 Mosquera, M. Photoinduced Proton and Charge Transfer in 2-(2'-Hydroxyphenyl)imidazo[4,5-
13 b]pyridine. *J. Phys. Chem. B* **2013**, *117*, 884-896.
- 14 (62) Carlotti, B.; Consiglio, G.; Elisei, F.; Fortuna, C. G.; Mazzucato, U.; Spalletti, A.
15 Intramolecular Charge Transfer of Push-Pull Pyridinium Salts in the Singlet Manifold. *J. Phys.*
16 *Chem. A* **2014**, *118*, 3580-3592.
- 17 (63) Young, J. W.; Vaquero-Vara, V.; Yi, J. T.; Pratt, D. W.; Moreno-Vargas, G.; Alvarez-
18 Valtierra, L. Using High Resolution Electronic Spectroscopy to Probe the Effects of Ring Twist
19 on Charge Transfer in 2-Phenylindole and N-Phenylcarbazole. *Phys. Chem. Chem. Phys.* **2013**,
20 *15*, 10251-10257.
- 21 (64) Thomas, J. A.; Young, J. W.; Fleisher, A. J.; Alvarez-Valtierra, L.; Pratt, D. W. Stark-
22 Effect Studies of 1-Phenylpyrrole in the Gas Phase. Dipole Reversal upon Electronic Excitation.
23 *J. Phys. Chem. Lett.* **2010**, *1*, 2017-2019.
- 24 (65) Fleisher, A. J.; Bird, R. G.; Zaleski, D. P.; Pate, B. H.; Pratt, D. W. High-Resolution
25 Electronic Spectroscopy of the Doorway States to Intramolecular Charge Transfer. *J. Phys.*
26 *Chem. B* **2013**, *117*, 4231-4240.
- 27 (66) Letrun, R.; Koch, M.; Dekhtyar, M. L.; Kurdyukov, V. V.; Tolmachev, A. I.; Rettig, W.;
28 Vauthey, E. Ultrafast Excited-State Dynamics of Donor-Acceptor Biaryls: Comparison between
29 Pyridinium and Pirylium Phenolates. *J. Phys. Chem. A* **2013**, *117*, 13112-13126.
- 30 (67) Dash, N.; Chipem, F. A.; Krishnamoorthy, G. Encapsulation of 2-(4'-N,N-
31 Dimethylamino)phenylimidazo[4,5-b]pyridine in Beta-Cyclodextrin: Effect on H-bond-Induced
32 Intramolecular Charge Transfer Emission. *Photochem. Photobiol. Sci.* **2009**, *8*, 1708-1715.
- 33 (68) Dash, N.; Krishnamoorthy, G. Modulation of the Photophysics of 2-(4'-N,N-
34 Dimethylaminophenyl)imidazo[4,5-b]pyridine by Long Chain N-alkylations. *Photochem.*
35 *Photobiol. Sci.* **2011**, *10*, 939-946.
- 36 (69) Mishra, A.; Sahu, S.; Dash, N.; Behera, S. K.; Krishnamoorthy, G. Double Proton
37 Transfer Induced Twisted Intramolecular Charge Transfer Emission in 2-(4'-N,N-
38 Dimethylaminophenyl)imidazo[4,5-b]pyridine. *J. Phys. Chem. B* **2013**, *117*, 9469-9477.
- 39 (70) Grabowski, Z. R.; Rotkiewicz, K.; Rettig, W. Structural Changes Accompanying
40 Intramolecular Electron Transfer: Focus on Twisted Intramolecular Charge-Transfer States and
41 Structures. *Chem. Rev.* **2003**, *103*, 3899-4031.
- 42 (71) Siemiarz, A.; Ware, W. R. Complex Excited-State Relaxation in p-(9-anthryl)-N,N-
43 Dimethylaniline Derivatives Evidenced by Fluorescence Lifetime Distributions. *J. Phys. Chem.*
44 **1987**, *91*, 3677-3682.
- 45 (72) Van der Meer, M. J.; Zhang, H.; Glasbeek, M. Femtosecond Fluorescence Upconversion
46 Studies of Barrierless Bond Twisting of Auramine in Solution. *J. Chem. Phys.* **2000**, *112*, 2878-
47 2887.
- 48
49
50
51
52
53
54
55
56
57
58
59
60

1
2
3 (73) Rafiq, S.; Sen, P. Spectroscopic Evidence of the Presence of an Activation Barrier in the
4 Otherwise Barrierless Excited State Potential Energy Surface of Auramine-O: A Femtosecond
5 Fluorescence Up-Conversion Study. *J. Chem. Phys.* **2013**, *139*, 124302.

6
7 (74) Amdursky, N.; Erez, Y.; Huppert, D. Molecular Rotors: What Lies Behind the High
8 Sensitivity of the Thioflavin-T Fluorescent Marker. *Acc. Chem. Res.* **2012**, *45*, 1548-1557.

9 (75) Marcus, Y.: *The Properties of Solvents*; John Wiley & Sons: Chichester, 1998.

10 (76) Lide, D. R.: *Handbook of Chemistry and Physics: A Ready-Reference of Chemical and*
11 *Physical Data*; 85th ed.; CRC Press LLC: Boca Raton, 2004.

12 (77) Katritzky, A. R.: *Handbook of Heterocyclic Chemistry*; Pergamon Press New York, 1985.
13
14
15
16
17
18
19
20
21
22
23
24
25
26
27
28
29
30
31
32
33
34
35
36
37
38
39
40
41
42
43
44
45
46
47
48
49
50
51
52
53
54
55
56
57
58
59
60

For Table of Contents Only

